NASA TECHNICAL NOTE

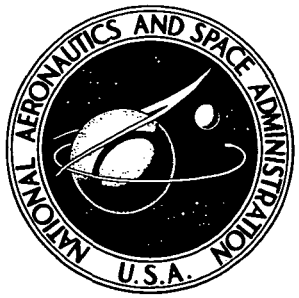

NASA TN D-7380

FATIGUE-TEST ACCELERATION WITH FLIGHT-BY-FLIGHT LOADING AND HEATING TO SIMULATE SUPERSONIC-TRANSPORT OPERATION

by L. A. Imig and L. E. Garrett

Langley Research Center

Hampton, Va. 23665

NATIONAL AERONAUTICS AND SPACE ADMINISTRATION • WASHINGTON, D. C. • DECEMBER 1973

1. Report No.	2. Government Accession No.	3. Recipient's Catalog No.
NASA TN D-7380		

4. Title and Subtitle	5. Report Date
FATIGUE-TEST ACCELERATION WITH FLIGHT-BY-FLIGHT LOADING AND HEATING TO SIMULATE SUPERSONIC-TRANSPORT OPERATION	December 1973
	6. Performing Organization Code
7. Author(s)	8. Performing Organization Report No.
L. A. Imig and L. E. Garrett	L-8992
	10. Work Unit No.
9. Performing Organization Name and Address	501-22-02-01
NASA Langley Research Center Hampton, Va. 23665	11. Contract or Grant No.
	13. Type of Report and Period Covered
12. Sponsoring Agency Name and Address	Technical Note
National Aeronautics and Space Administration Washington, D.C. 20546	14. Sponsoring Agency Code

15. Supplementary Notes

16. Abstract

Possibilities for reducing fatigue-test time for supersonic-transport materials and structures were studied in tests with simulated flight-by-flight loading. In order to determine whether short-time tests were feasible, the results of accelerated tests (2 sec per flight) were compared with the results of real-time tests (96 min per flight). The effects of design mean stress, the stress range for ground-air-ground cycles, simulated thermal stress, the number of stress cycles in each flight, and salt corrosion were studied. The flight-by-flight stress sequences were applied to notched sheet specimens of Ti-8Al-1Mo-1V and Ti-6Al-4V titanium alloys. A linear cumulative-damage analysis accounted for large changes in stress range of the simulated flights but did not account for the differences between real-time and accelerated tests. The fatigue lives from accelerated tests were generally within a factor of two of the lives from real-time tests; thus, within the scope of the investigation, accelerated testing seems feasible.

17. Key Words (Suggested by Author(s))	18. Distribution Statement
Fatigue (materials) Titanium alloys Elevated temperature Flight simulation Supersonic transports	Unclassified – Unlimited

19. Security Classif. (of this report)	20. Security Classif. (of this page)	21. No. of Pages	22. Price*
Unclassified	Unclassified	51 48	Domestic, $3.00 Foreign, $5.50

*For sale by the National Technical Information Service, Springfield, Virginia 22151

FATIGUE-TEST ACCELERATION WITH FLIGHT-BY-FLIGHT LOADING AND HEATING TO SIMULATE SUPERSONIC-TRANSPORT OPERATION

By L. A. Imig and L. E. Garrett
Langley Research Center

SUMMARY

Possibilities for reducing fatigue-test time for supersonic-transport materials and structures were studied in tests with simulated flight-by-flight loading. In order to determine whether short-time tests were feasible, the results of accelerated tests (2 sec per flight) were compared with the results of real-time tests (96 min per flight). The effects of design mean stress, the stress range for ground-air-ground cycles, simulated thermal stress, the number of stress cycles in each flight, and salt corrosion were studied. The flight-by-flight stress sequences were applied to notched sheet specimens of Ti-8Al-1Mo-1V and Ti-6Al-4V titanium alloys. A linear cumulative-damage analysis accounted for large changes in stress range of the simulated flights but did not account for the differences between real-time and accelerated tests. The fatigue lives from accelerated tests were generally within a factor of two of the lives from real-time tests; thus, within the scope of the investigation, accelerated testing seems feasible.

INTRODUCTION

Fatigue tests of commercial supersonic-transport airplanes will probably be necessary to derive confidence in the long-time structural integrity of such airplanes. The fatigue test must account for the time-dependent effects of elevated temperature and stress. A very complex test is being conducted to satisfy these requirements for the British-French *Concorde*; this very costly fatigue test has a planned duration of nearly 7 years. (See ref. 1.) Because of the great expense associated with such a test, simplified, accelerated procedures are needed. A previous attempt to accelerate fatigue tests by replacing representative cyclic stresses, temperatures, and times with "equivalent conditions" obtained by larger stresses and temperatures for fewer cycles and shorter times achieved only limited success. (See ref. 2.)

The objective of the present effort is to determine the relations between the results of "real-time" and "accelerated" fatigue tests of simple specimens. These relationships must be known if accelerated tests are to retain the essential features from the real-time operation of a supersonic transport. The present study was limited to tests of titanium alloys potentially useful for a supersonic transport operating at Mach 3. The materials were duplex-annealed Ti-8Al-1Mo-1V, annealed Ti-6Al-4V, and solution treated and

aged (STA) Ti-6Al-4V. Test specimens were notched to represent a structural region containing a moderate stress concentration.

Stresses representative of those expected at a critical location in a lower wing skin and the temperature associated with flight at Mach 3 were programed to simulate individual flights for both real-time and accelerated fatigue tests. Real-time tests included a 90-minute-long elevated temperature cycle in each flight to simulate the temperature induced by supersonic cruise, and each flight required about 96 minutes to complete. In contrast, accelerated tests were conducted at room temperature or at constant elevated temperature, and each flight required only about 2 seconds to complete. A linear cumulative-damage analysis was conducted for tests of Ti-8Al-1Mo-1V.

Previous results of this study were presented in references 3 to 5; this report contains previous results and additional, more recent data.

SYMBOLS

The units for physical quantities used in this paper are given in the International System of Units (SI); however, measurements during the investigation were made in U.S. Customary Units. Factors relating these two systems of units are given in reference 6; those pertinent to the present investigation are presented in appendix A.

K_{exp}	experimentally determined elastic-stress concentration factor
n	number of stress cycles applied at given stress level
N	number of stress cycles required to cause failure at given stress level
S_{max}	maximum net-section nominal stress, MN/m^2
θ	ratio of stress amplitude to design mean stress

EXPERIMENTAL PROCEDURES

Materials and Specimens

The sheet materials for this investigation were from three heats of duplex-annealed Ti-8Al-1Mo-1V, 1.27 mm thick; one heat of annealed Ti-6Al-4V, 1.02 mm thick; and one heat of solution treated and aged Ti-6Al-4V, 1.27 mm thick. The heat treatments of the materials are given in table I and their chemical compositions are presented in table II.

Fatigue specimens from all three materials were made to the configurations shown in figure 1. The longest dimension of all specimens was alined with the rolling direction of the sheet material. As shown in figure 1, specimens for accelerated tests had one notch whereas the specimen for real-time tests had six notches. With the multiple-notch configuration, multiple test data were obtained from a single test. The multiple-notch specimens were spliced after each failure; the test was then resumed until all notches had failed. The notches in the specimens had stress concentration factors of 4.1 to represent a structural region containing a moderate stress concentration. Details of machining the specimens are presented in appendix B. The tensile properties of all three materials were determined by tests of standard tensile specimens at room temperature, 561 K, and 616 K. Tensile-test procedures are presented in appendix B.

Stresses for Fatigue Tests

Gust loads for an assumed supersonic transport were derived from a mathematical model of atmospheric turbulence (ref. 7). Maneuver loads were based on data from current subsonic airplanes. The stresses from the gust and maneuver loads were combined to form a stress spectrum for the assumed supersonic airplane. (See ref. 3.) Programed stresses simulated individual flights for both real-time and accelerated tests, as shown in figure 2. The design mean stress in figure 2 represents a stress in the lower wing skin during level unaccelerated flight at maximum airplane mass. All stress amplitudes are normalized to the design mean stress.

During the real-time tests, figure 2(a), a 90-minute-long elevated temperature cycle in each flight simulated the heating induced by supersonic cruise; each flight lasted about 96 minutes. In contrast, accelerated tests were conducted at room temperature or at constant elevated temperature, and each flight lasted only about 2 seconds (fig. 2(b)). The stress amplitudes and numbers of cycles were identical in both real-time and accelerated tests. The flights shown in figures 2(a) and 2(b) simulate commercial operation. Such flights will be referred to as operational flights. The important aspects of these flights are that more stress cycles occurred during climb than during cruise or descent, that the mean stress decreased throughout the flight to simulate a loss of mass due to fuel usage, and that a compressive stress excursion occurred at the end of each flight to complete the ground-air-ground transition (GAG).

The techniques for programing the stress are described in reference 3; briefly, the stress amplitudes calculated to occur at least once per flight were grouped together to form a basic operational flight. (See figs. 2(a) and 2(b).) Larger stress amplitudes, calculated to occur less frequently than one per flight, were added during each 5th, 100th,

1000th, and 10 000th flight. These flights were of increasing severity. Figure 2(c) shows a 10 000th operational flight for an accelerated test.

Check flights, shown in figure 2(d), represented flights for crew training and were inserted in all tests after each group of 24 operational flights. Each check flight included seven GAG cycles to represent the touch-and-go landings that occur frequently during check flying. Infrequently occurring severe stresses were added to 10th and 100th check flights. For accelerated tests, check flights were applied at the same constant temperature used for operational flights. For real-time tests, check flights were applied at room temperature. The stress at 1g for all check flights was seven-tenths of the design mean stress, as shown in figure 2(d).

Test Parameters

The test parameters studied were simulated thermal stress, minimum stress for GAG cycles, and number of stress cycles in each flight. These parameters were incorporated into tests by modifying operational flights, as shown in figure 3. The boxes in figure 3(a) represent the stress cycles for the climb, cruise, and descent segments of operational flights. The letters in the boxes identify the sequences of mean stress for each of the parameters studied. For type-A and type-E stress sequences the ratios of mean stress to the design mean stress for climb, cruise, and descent were 1.00, 0.75, and 0.60, respectively. The minimum stress for type-A sequences was -0.50 of the design mean stress. Those sequences with a minimum stress of zero were designated E_0 and those with a minimum stress of -1g were designated E_1. Type-C sequences had stress ratios of 1.00, 1.35, and 0.20 for climb, cruise, and descent, respectively. The minimum stress for type-C sequences was -0.50 of the design mean stress. The effect of repeated applications of salt solution on fatigue life was studied in another series of tests using a type-A stress sequence.

Tests to evaluate these parameters were conducted at design mean stresses of 172, 207, and 241 MN/m^2. Each of the stress sequences is discussed further in the following paragraphs.

Type-A stress sequences (reference).- The type-A stress sequence represents the derived operational flight described in the previous section. It served as a reference test condition. Tests with type-A stress sequences were conducted on all three materials in both real-time and accelerated tests.

Type-C stress sequence (thermal stress).- The effects of thermal stress in subsurface structure were determined in tests with type-C sequences. The mean stresses for cruise and descent were programed as shown in figure 3 (see boxes labeled C) to simulate the stresses induced by the cycle of aerodynamic heating and cooling that occurs

during each flight. Real-time and accelerated tests with type-C stress sequences were conducted on duplex-annealed Ti-8Al-1Mo-1V.

Type-E stress sequences (minimum stress for GAG cycles).- The effect of the minimum stress for GAG cycles was studied by conducting two series of tests. In one series the minimum stress was zero and in the other series the minimum stress was equal to the negative of the design mean stress. (See fig. 3.) These test results, and those with type-A stress sequences in which the minimum stress for GAG cycles was -0.50 of the design mean stress, provided data to assess the effect of the overall stress range during a flight. All tests with type-E stress sequences were accelerated and were conducted on duplex-annealed Ti-8Al-1Mo-1V with one exception, a real-time test with a minimum stress of zero for GAG cycles.

Type-F and type-G stress sequences (number of cycles per flight).- The effect of the number of stress cycles in each flight was evaluated in tests with type-F and type-G stress sequences. These tests were conducted to determine the feasibility of simplifying the tests by omitting cycles of selected small stress amplitudes. For type-F stress sequences, all stress cycles of the smallest amplitude were arbitrarily omitted. Because the cruise and descent segments of basic operational flights consisted entirely of cycles of the smallest amplitude, the resulting flight retained only seven stress cycles, all from the climb segment of flight, as shown in figure 3(b). Each 5th flight, 100th flight, and so forth, which contained the larger stress cycles in cruise and descent, retained the "normal" climb-cruise-descent sequence of flight segments.

Type-G stress sequences were synthesized by retaining only 1 cycle which ranged from the maximum stress in each flight to -0.50 of the design stress, as shown in figure 3(c). Tests with type-F and type-G stress sequences were conducted on Ti-8Al-1Mo-1V and Ti-6Al-4V, STA, in accelerated tests.

Salt corrosion.- A salt solution was applied to three specimens for real-time tests because of concern over the possible detrimental effect of hot-salt-stress corrosion on fatigue life. The salt was applied by wetting the specimens once each work day (normally 5 days per week) with a $3\frac{1}{2}$-percent solution of NaCl in distilled water. The maximum temperature in the real-time tests with salt was 616 K. Real-time and accelerated tests without salt were also conducted at 616 K to provide control data. All tests in this series were conducted on duplex-annealed Ti-8Al-1Mo-1V using type-A stress sequences.

Tests

Both the real-time and accelerated tests were conducted in closed-loop, servo-controlled, hydraulically actuated testing machines. The magnitudes of the axial loads were based on the net-section area of each specimen. Usually six fatigue lives were

obtained for each test condition in both real-time and accelerated tests; however, only three fatigue lives were obtained for accelerated tests with type-F and type-G stress sequences.

Stresses and temperatures for real-time tests were scheduled by a chart follower. The cruise segment of each flight included a 90-minute-long elevated-temperature cycle. At the end of the cruise segment, the heat source was turned off, compressed air cooled the specimens, and the descent segment of the simulated flight began. Thus, the stresses in descent were applied during a period of decreasing temperature. Typically, the temperature of the specimen was reduced to 320 K before the descent segment of flight was completed. The cooling continued for a short time into the climb segment of the succeeding flight until a minimum temperature of 300 K was reached.

Stresses for most of the accelerated tests were scheduled by punched cards. Tests were conducted at constant elevated temperature or constant room temperature. Each flight lasted about 7 seconds. The accelerated-test system was modified recently, and a computer scheduled the last series of loads. It permitted unattended operation 24 hours per day and applied each flight in about 2 seconds. All of the testing equipment is discussed in more detail in appendix B.

Cumulative-Damage Analysis

A linear cumulative-damage analysis (Miner's method, ref. 8) was conducted to assess whether the trends in fatigue life produced by the test parameters could be predicted. The analysis was conducted for tests of Ti-8Al-1Mo-1V using constant amplitude fatigue data from reference 3 for that material. The constant amplitude data were generated using specimens identical to those used in the present tests. Corresponding constant amplitude data for Ti-6Al-4V specimens were not available.

Life fractions (values of n/N) were calculated for each combination of alternating and mean stress for each test condition and were based on the median fatigue lives. The stress range for ground-air-ground cycles was assumed to be from the minimum to the maximum stress occurring in a given flight. For accelerated tests, the analysis used constant amplitude fatigue data at either room temperature or 561 K, as appropriate. For analysis of real-time tests, stress cycles in climb and descent were assumed to occur at room temperature; stress cycles for cruise were assumed to occur at 561 K. In real-time tests with type-C stress sequences, the compressive part of the ground-air-ground cycle occurred at a relatively low temperature as previously discussed, but the tensile part of the ground-air-ground cycle occurred during the elevated temperature cruise portion of flight. Because no constant amplitude data that include cyclic temperature are available, cumulative damage for the ground-air-ground cycle was calculated based on constant amplitude data at elevated temperature.

RESULTS AND DISCUSSION

General Observations

The longitudinal tensile properties of all three materials used in this investigation are presented in table III and are considered to be typical for these titanium alloys. Fatigue lives are presented in table IV for real-time tests and in tables V, VI, and VII for accelerated tests at room temperature, 561 K, and 616 K, respectively. The tables indicate the segment of flight, the kind of flight, and the amplitude of the load cycle in which failure occurred. In order to calculate the stress at failure, the mean stress for the segment of flight in which failure occurred must be added to the amplitude given in the tables; however, the amplitude of the cycle probably does not indicate the failure load accurately unless the peak of the cycle was reached just at failure.

All of the specimens failed during operational flights; within the operational flights, all failures occurred during a segment of flight having a higher mean stress than the preceding segment of flight, with only two exceptions.

The fatigue data are plotted in figures 4 to 9. The fatigue lives in the tables and figures are the total number of flights (operational and check) that were survived by test specimens before complete failure occurred; the median life for each series of tests is plotted in the figures.

As expected, a large systematic effect of design mean stress on fatigue life was observed for all test conditions, as shown in figures 4 to 9. For example, figure 4 indicates that fatigue lives from accelerated tests at 241 MN/m^2 were approximately an order of magnitude shorter than at 172 MN/m^2; the effect of design mean stress was similarly large for all three materials and for both real-time and accelerated tests.

Comparisons among the results of accelerated tests in figures 4 to 8 show that the lives at 561 K were about half the lives from room-temperature tests.

The relatively small differences between fatigue lives from real-time and accelerated tests suggest that accelerated tests can provide adequate estimates of the real-time fatigue lives. However, research on more complex specimens will be required before that tentative conclusion can be extended to structural prototypes.

Cumulative-Damage Analysis

Table VIII shows the calculated median values of $\sum \frac{n}{N}$ at failure, the portion of $\sum \frac{n}{N}$ at failure due to GAG cycles in operational flights, and the predicted fatigue lives. As shown in table VIII, the 41 values of $\sum \frac{n}{N}$ ranged from 0.12 to 1.60; the median value was 0.56 and all but seven values were less than 1.00.

The ground-air-ground cycles in operational flights produced most of the calculated fatigue damage for all of the test conditions (50 percent to 97 percent of the total). Because ground-air-ground cycles were the predominant source of damage, and because high ground-air-ground stress cycles result in less scatter than do small ones in constant amplitude data, more reliable cumulative damage calculations should be expected for tests at high mean stresses than for low mean stresses; accordingly, study of the values of $\sum \frac{n}{N}$ in table VIII indicates median values of $\sum \frac{n}{N}$ of 0.51, 0.58, and 0.67 for tests at design mean stresses of 172, 207, and 241 MN/m^2, respectively. Unfortunately, the least accurate prediction occurs for the most practical design condition (low mean stress) for structures intended to have long service lives.

In most cases, the values of $\sum \frac{n}{N}$ for tests in which smaller amplitudes were deleted (type F and type G) were larger than the values for tests that included all the "in-flight" loads (type A, type C, and type E) in accelerated tests at both temperatures. The progressive flight simplification (type A to type F to type G) produced flights tending toward constant amplitude ground-air-ground cycles; because the ground-air-ground cycles were the predominant source of damage, the values of $\sum \frac{n}{N}$ increased progressively with the flight simplification.

The predicted lives for tests at elevated temperature were generally shorter than for room-temperature tests as might be expected from the relative positions of the S-N curves for room and elevated temperature in the region of high stresses. (The S-N curves for room and elevated temperature intersect, see ref. 3.) The experimental lives for the tests at elevated temperature were also shorter than for the room-temperature tests, but the differences between experimental lives were larger than would be anticipated from the linear damage analysis; thus, predicted lives were less accurate for tests at elevated temperature than for tests at room temperatures.

The predicted lives shown in table VIII are plotted in the figures along with the corresponding experimental lives.

Effect of Test Parameters

In general, parameters that caused larger stress ranges for the simulated flights produced shorter fatigue lives. Tests with each of the stress sequences are discussed in the following paragraphs.

Reference tests (type-A stress sequence).- The results for type-A stress sequences are shown in figure 4 for both real-time and accelerated tests of all three materials. At the two higher design mean stresses (241 and 207 MN/m^2), most of the lives from real-time tests were bracketed by the lives from accelerated tests at room and elevated temperature. The median real-time life for Ti-8Al-1Mo-1V at 172 MN/m^2 was shorter than the life from the corresponding accelerated tests at elevated temperature. The real-time test of Ti-6Al-4V, STA, at 172 MN/m^2 has produced only one failure with a shorter life than for the corresponding accelerated tests at elevated temperature. Thus, the design mean stress influenced the relations between the real-time and accelerated fatigue lives. Such a variable relationship suggests that a range of stress levels (or other parameter) should be employed for accelerated tests to identify trends and prevent misleading interpretations; alternatively, if the investigation is constrained to few tests, the tests should simulate very closely the actual operating conditions.

The cumulative-damage analysis correctly predicted the order of the fatigue lives for each design mean stress but did not account for the differences between real-time and accelerated test results.

Effect of simulated thermal stress (type-C stress sequence).- The results of real-time and accelerated tests in which simulated thermal stresses were employed are shown in figure 5. In contrast to the results with the reference (type-A) stress sequence shown in figure 4, the real-time fatigue lives from this series were longer than those from the corresponding accelerated tests at room or elevated temperature.

As expected, the fatigue lives from accelerated tests with the type-C stress sequence were somewhat shorter than the lives for the type-A stress sequence, as shown in figure 6(a). The shorter lives for tests with the type-C stress sequence were undoubtedly due to the high maximum stresses applied during the cruise segments of basic, 5th, and 100th flights. Somewhat surprisingly, the lives for real-time tests with type-C stress sequences were longer than the lives from real-time tests with type-A stress sequences, as shown in figure 6(b). These unexpected results are not well understood; however, a detailed analysis of the local stresses for the type-A and type-C real-time stress sequences should provide a better understanding. Such an analysis was beyond the scope of the present effort.

Effect of minimum stress for GAG cycles (type-E stress sequences).- The minimum stress for GAG cycles had a large influence on fatigue life in tests at all three design mean stresses, as shown in figure 7. For example, at a design mean stress of 207 MN/m^2 the fatigue lives for room-temperature tests with a minimum stress of -207 MN/m^2 were less than one-sixth those with a minimum stress of zero; tests at other values of design mean stress produced similarly large effects on fatigue lives. The minimum stress in the lower wing skin, which occurs at the end of the GAG cycle, depends largely on the

landing-gear location, the stiffness of the wing, and the wing mass distribution. The importance of the minimum stress in design is evident from the large differences in fatigue life shown in figure 7.

In contrast to all other test conditions, when the minimum stress was zero, the cumulative-damage analysis predicted longer fatigue lives at elevated temperature than at room temperature. The stresses associated with these ground-air-ground cycles fall in a region of constant-amplitude data where the lives for tests at elevated temperature were longer than for tests at room temperature, and, of course, the predictions reflect this trend in the constant-amplitude data. The test results did not show this predicted trend.

In general, the predictions accounted for the different minimum stresses in this series of tests.

Effect of the number of cycles per flight (type-F and type-G stress sequences).- Tests in which small stress cycles were eliminated from each simulated flight produced fatigue lives that were longer than the lives for tests with the reference (type-A) sequence, as shown in figure 8. Although the number of flights required to fail the specimen was larger in tests with type-F and type-G stress sequences than for type-A stress sequence, the test time was shorter because the flights contained fewer cycles. Thus, important savings of testing time are possible by using simplified flights. Such an approach should be considered carefully before applying it to the fatigue test of an airplane or a complex component because the failure locations in the structure that are identified by a simplified test might be different from those identified by a more realistic sequence of flight stresses (see, for examples, refs. 9 to 11). Thus, a misleading result might be obtained from an inappropriately simplified test. Also, as shown in figure 8, the cumulative-damage analysis did not account for the longer lives.

Tests with salt corrosion (type-A stress sequence).- The results of real-time tests to determine the effect of salt corrosion are shown in figure 9, along with the results of related real-time and accelerated tests. The maximum temperature in this series of tests was 616 K to exaggerate the effect of the salt environment. The total exposure to the salt and elevated temperature exceeded 5000 hours in all of the real-time tests. As expected, the fatigue lives were systematically shorter for the systematically more severe test environments; however, the results shown in figure 9 indicate that the salt had only a relatively small effect on fatigue life. In contrast, reference 12 indicated that hot-salt-stress-corrosion cracking occurred in duplex-annealed Ti-8Al-1Mo-1V after only 800 to 1200 hours of exposure to 590 K with heavy salt coatings and constant stresses equal to the cruise levels in the present tests. Thus, quantitative investigations of hot-salt-stress corrosion should employ realistic simulations of the salt environment.

Correlation of Test Results

The correlation of fatigue life with maximum stress is shown in figure 10 for accelerated tests. The maximum stress in each basic flight for stress sequences of types A, C, and D was plotted against the corresponding fatigue life. (The type-D stress sequence simulates the thermal stress in a lower wing skin; fatigue data are from ref. 3.) The good correlation shown in figure 10 probably resulted from using a single distribution of gust and maneuver amplitudes for all the tests. Similar correlations could probably be obtained independently from tests based on other distributions of stress amplitudes but should not be expected for tests based on two or more distributions. This type of correlation remains to be determined for tests of complex structures or structural components.

The fatigue lives from real-time tests are shown in figure 11, along with the faired curve for accelerated tests from figure 10. The lives indicated by the curve are shorter than those for real-time tests with type-C stress sequences (thermal stress for subsurface structure) but are longer than for real-time tests with type-A stress sequences (no thermal stress). Because supersonic-transport operation will produce elevated temperature and thermal stress, the real-time test results with type-C stress sequences are more relevant to a structural condition than tests with type-A stress sequences. Based on figure 11, the use of accelerated tests to estimate real-time fatigue lives appears promising; however, extension of this concept to built-up structures is as yet undetermined.

CONCLUSIONS

This investigation was conducted to study ways of reducing testing time for structural materials suitable for supersonic-transport airplanes. Similar investigations employing structural components will be required to develop viable accelerated tests for supersonic-transport structures.

For the present effort, stresses representing the flight-by-flight operation of a supersonic (Mach 3) transport airplane were applied to test specimens in real-time tests and in accelerated tests. Tests with these stress sequences determined the effects on fatigue life of simulated thermal stress, the minimum stress for ground-air-ground (GAG) cycles, and the number of stress cycles for each simulated flight. In addition, a salt solution was applied daily to some of the specimens in the real-time tests to assess the effect of salt-stress corrosion.

The test program was conducted with notched specimens made of three sheet materials: Ti-8Al-1Mo-1V, duplex-annealed; Ti-6Al-4V, annealed; and Ti-6Al-4V, solution treated and aged. The results of the investigation suggest that real-time fatigue lives of these titanium alloys (under conditions simulating flight at Mach 3) can be adequately estimated by data from accelerated tests. Other, more detailed, observations are:

1. In general, parameters that caused larger stress ranges for the simulated flights produced shorter fatigue lives.

2. Fatigue lives from accelerated tests were correlated by the maximum stresses that occurred in the basic operational flights.

3. The fatigue lives from accelerated tests at 561 K were about one-half the lives at room temperature for all three materials.

4. Systematic simplification of tests, produced by omitting stress cycles, produced systematically longer fatigue lives.

5. In real-time fatigue tests of Ti-8Al-1Mo-1V at 616 K, a daily application of $3\frac{1}{2}$-percent NaCl solution had little detrimental effect on the fatigue lives.

6. The linear cumulative-damage analysis accounted for differences in fatigue lives due to large changes in stress range but did not account for the differences between real-time and accelerated tests.

Langley Research Center,
National Aeronautics and Space Administration,
Hampton, Va., September 20, 1973.

APPENDIX A

CONVERSION OF THE INTERNATIONAL SYSTEM OF UNITS TO U.S. CUSTOMARY UNITS

The International System of Units (SI) was adopted by the Eleventh General Conference on Weights and Measures, Paris, October 1960. Conversion factors for the units used herein are from reference 6 and are presented in the following table:

Physical quantity	SI Unit	Conversion factor (*)	U.S. Customary Unit
Frequency	hertz (Hz)	1.0	cps
Force	newtons (N)	0.2248	lbf
Length	meters (m)	39.37	in.
Stress	newtons/meter^2 (N/m^2)	1.45×10^{-7}	ksi = 1000 lbf/in^2
Temperature	kelvin (K)	$^{o}F = \frac{9}{5}$ (K-255.4)	^{o}F

*Multiply value given in SI Units by conversion factor to obtain equivalent value in U.S. Customary Units or apply conversion formula.

Prefixes to indicate multiples of SI units are as follows:

Prefix	Multiple
milli (m)	10^{-3}
centi (c)	10^{-2}
kilo (k)	10^{3}
mega (M)	10^{6}
giga (G)	10^{9}

APPENDIX B

PROCEDURES AND TEST EQUIPMENT

Specimens

Standard tensile specimens with test sections 1.27 cm wide and 6.3 cm long were used to determine the tensile properties of the materials. The configurations of fatigue specimens are shown in figure 1. Specimens for accelerated tests had one notched test section and specimens for real-time tests had six notched test sections. The longitudinal dimension of all specimens was parallel to the rolling direction of the sheet materials; specimen surfaces were left as rolled. Notches in the specimen had experimentally determined elastic-stress concentration factors of 4.1. The notch configuration shown in the figure simulates a theoretical ellipse having the same major and minor axes and with the same minimum radius of curvature. The dimensions of the theoretical ellipse were determined by a procedure developed in reference 13. The notch in the specimens was generated by drilling two small holes in a three-step process; an undersized hole with a 2.79-mm diameter was drilled first and enlarged by increasing the drill diameter in increments of 0.076 mm to achieve the final diameter of 2.94 mm. The material between the two small holes was then removed by drilling with a 6.36-mm-diameter drill. The small burrs produced by the drilling operation were removed by holding the specimen lightly against a rotating rubber rod that was impregnated with an abrasive. The rod was sharpened to a conical point; thus, the deburring operation resulted in a slight bevel around the ends of the notch.

Tensile Tests

Tensile tests were conducted in a universal hydraulic testing machine which has a 530-kN capacity. Stress-strain curves were obtained autographically with an x-y plotter. The electronic signal from a load cell in series with the specimen actuated the recorder drive for the stress axis. The strain axis was actuated by the output of an extensometer that incorporated a linear variable differential transformer. The extensometer was attached to the specimen in the reduced section and had a gage length of 25.4 mm. The elongation in 50.8 mm was determined by measuring the distance, after fracture, between grid lines placed on each specimen prior to the test.

Fatigue Tests

All specimens were loaded axially and stresses were based on the initial net area of each specimen at its minimum section.

Two types of closed-loop electrohydraulic servosystem were employed for accelerated tests. In one system the loads were scheduled by punched cards, as described in reference 14. During the investigation, the testing system was modified by changing the mode of load scheduling from the use of a large volume of prepunched cards to automatic control by means of a small computer. The operation of the testing system remained basically the same, but the modification resulted in much faster operation and allowed unattended operation around the clock. At the time of the modification, the number of testing stations was increased to four from the previous three, thereby adding more testing capacity to the system. A schematic drawing of the modified system for one testing station is shown in figure 12.

In operation, the computer selects each load level for application to the specimen, as shown in figure 12. As a result of that load, the weighbar generates an electrical feedback opposing the command signal from the computer. When the feedback and command signals have canceled each other (within an adjustable tolerance), the comparator instructs the computer to advance to the next load level. The electrical characteristics of the system allow relatively high operating speeds depending on the load levels being applied; an average operating speed of about 30 Hz was achieved in the present investigation. The accuracy of load application during operation has been determined to be within ±0.2 percent of weighbar capacity (44 kN).

The real-time tests were conducted in a series of 10 closed-loop electrohydraulic servosystems. As shown schematically in figure 13, the loads were scheduled by a chart follower. As the probe moves along the loading trace, the slidewire resistor transmits a varying electrical signal to the servovalve. The electrical feedback from the load cell limits the loading to the desired value as in the systems for accelerated tests. Unlike the systems for accelerated tests, the real-time test system does not automatically ensure that the desired load was reached before applying a subsequent load because the chart rotates at a constant speed. Thus, the length of the loading trace at the maximum value of each load cycle must be sufficient to allow time for probe travel and servohydraulic response so that the required loads are applied to the specimen. For the real-time tests of this investigation, charts were prepared so that stress cycles with amplitudes θ less than 0.54 were applied at 1/4 Hz. Cycles with amplitudes θ of 0.54, and greater, were applied at 1/8 Hz.

As shown in figure 13, parallel darkened bands were located along one edge of the chart. The dark bands prevent light from reflecting to photosensitive diodes. In regions where the bands are interrupted, the diodes activate either the temperature controller or the compressed-air supply in synchronization with the flight loads, as desired.

REFERENCES

1. Ripley, E. L.: The Philosophy Which Underlies the Structural Tests of a Supersonic Transport Aircraft With Particular Attention to the Thermal Cycle. Advanced Approaches to Fatigue Evaluation, NASA SP-309, 1972, pp. 1-91.

2. Dill, H. D.; and Newman, J. A.: Experimental Verification of the Suitability of Compressing the Time of Mission Profile During Elevated Temperature Fatigue Testing. AFFDL-TR-70-113, U.S. Air Force, Feb. 1971.

3. Imig, L. A.; and Illg, Walter: Fatigue of Notched Ti-8Al-1Mo-1V Titanium Alloy at Room Temperature and 550° F (560° K) with Flight-by-Flight Loading Representative of a Supersonic Transport. NASA TN D-5294, 1969.

4. Imig, L. A.: An Investigation of Fatigue in a Supersonic Transport Operating Environment. Paper No. 700033, Soc. Automot. Eng., Jan. 1970.

5. Imig, L. A.: Fatigue of SST Materials Using Simulated Flight-by-Flight Loading. Fatigue at Elevated Temperatures, Spec. Tech. Publ. No. 520, Amer. Soc. Testing Mater., 1973.

6. Comm. on Metric Pract.: ASTM Metric Practice Guide. NBS Handbook 102, U.S. Dep. Com., Mar. 10, 1967.

7. Press, Harry; and Steiner, Roy: An Approach to the Problem of Estimating Severe and Repeated Gust Loads for Missile Operations. NACA TN 4332, 1958.

8. Miner, Milton A.: Cumulative Damage in Fatigue. J. Appl. Mech., vol. 12, no. 3, Sept. 1945, pp. A-159 – A-164.

9. Mann, J. Y.: Fatigue Testing – Objectives, Philosophies and Procedures. ARL SM Rep. 336, Dep. Supply, Aust. Def. Sci. Serv., Feb. 1972.

10. Huston, Wilber B.; and Ward, John F.: Evaluation of Fatigue Sensitive Areas and Cumulative Damage in Full-Scale Fatigue Testing. Proceedings of the Symposium on Fatigue of Aircraft Structures, WADC TR 59-507, U.S. Air Force, Aug. 1959, pp. 919-946.

11. Peterson, John J.: Fatigue Behavior of Ti-8Al-1Mo-1V Sheet in a Simulated Wing Structure Under the Environment of a Supersonic Transport. NASA CR-333, 1965.

12. Royster, Dick M.: Hot-Salt-Stress-Corrosion Cracking and Its Effect on Tensile Properties of Ti-8Al-1Mo-1V Titanium-Alloy Sheet. NASA TN D-4674, 1968.

13. McEvily, Arthur J., Jr.; Illg, Walter; and Hardrath, Herbert F.: Static Strength of Aluminum-Alloy Specimens Containing Fatigue Cracks. NACA TN 3816, 1956.

14. Naumann, Eugene C.: Evaluation of the Influence of Load Randomization and of Ground-Air-Ground Cycles on Fatigue Life. NASA TN D-1584, 1964.

TABLE I.- HEAT TREATMENTS FOR TITANIUM ALLOYS

[Information supplied by manufacturers]

Alloy	Treatment
Ti-8Al-1Mo-1V, duplex annealed	Annealed at 1060 K for 8 hours, furnace cooled; annealed at 1060 K for 15 minutes, air cooled
Ti-6Al-4V, annealed	Annealed at 1080 K for 1 hour, furnace cooled to 980 K, air cooled
Ti-6Al-4V, solution treated and aged	Solution treated at 1190 K for 9 minutes, water quenched; aged at 950 K for 4 hours, air cooled

TABLE II.- CHEMICAL COMPOSITIONS OF TITANIUM ALLOYS

[Information supplied by manufacturers]

Mill heat	Weight percentage of –								
	Al	C	Fe	H	Mo	N	O	V	Ti
Ti-8Al-1Mo-1V, duplex annealed									
I	7.9	0.026	0.11	0.003 to 0.006	1.1	0.011		1.0	Balance
II	7.8	.025	.07	.008 to .009	1.1	.010		1.0	Balance
III	7.8	.025	.05	.010 to .011	1.1	.012		1.0	Balance
Ti-6Al-4V, annealed									
IV	6.1	0.026	0.15	0.011		0.013		4.0	Balance
Ti-6Al-4V, solution treated and aged									
V	6.2	0.02	0.17	(a)		0.010	0.123	4.4	Balance

[a]50 parts per million.

TABLE III.- LONGITUDINAL TENSILE PROPERTIES OF TITANIUM-ALLOY SHEET MATERIALS

Mill heat	Ultimate tensile strength, MN/m^2	Tensile yield strength at 0.2-percent offset, MN/m^2	Young's modulus, GN/m^2	Elongation in 50.8 mm, percent
(a) Ti-8Al-1Mo-1V, duplex annealed, 1.27 mm thick				
Properties at room temperature				
I	1027	933	117	12.6
II	994	910	119	12.3
III	1002	918	123	14.8
Properties at 561 K				
I	816	679	110	11.2
Properties at 616 K				
I	796	636	104	11.0
(b) Ti-6Al-4V, annealed, 1.02 mm thick				
Properties at room temperature				
IV	1034	961	114	13.1
Properties at 561 K				
IV	744	641	114	9.4
Properties at 616 K				
IV	733	650	107	8.3
(c) Ti-6Al-4V, solution treated and aged, 1.27 mm thick				
Properties at room temperature				
V	1034	1009	120	14.8
Properties at 561 K				
V	792	688	113	10.7
Properties at 616 K				
V	761	653	112	9.9

TABLE IV.- FATIGUE LIVES FROM REAL-TIME TESTS

[Notched specimens, $K_{exp} = 4.1$]

(a) Duplex-annealed Ti-8Al-1Mo-1V titanium-alloy sheet, 1.27 mm thick

Stress sequence	Design mean stress, MN/m^2	Minimum stress for GAG cycles, MN/m^2	Specimen failed at –			Fatigue life, flights	
			θ	Segment of flight	Kind of flight	Individual	Median (a)
A	172	-86	0.44	Climb	5	14 858	[b]19 014
			.54	Climb	100	15 978	
			.44	Climb	5	19 014	
			(c)	(c)	(c)	[c]>19 014	
			(c)	(c)	(c)	[c]>19 014	
	207	-104	0.44	Climb	5	8 686	10 050
			.44	Climb	5	8 727	
			.64	Climb	100	9 681	
			1.04	Climb	10 000	10 420	
			.64	Climb	100	17 394	
			(d)	(d)	(d)	[d]>23 500	
	241	-120	0.64	Climb	100	4 510	5 093
			.44	Climb	5	4 748	
			.64	Climb	100	5 024	
			.34	Climb	Basic	5 162	
			.84	Climb	1 000	5 202	
			.74	Climb	1 000	5 202	
[e]A	172	-86	(f)	(f)	(f)	(f)	(f)
	207	-104	0.44	Climb	5	6 056	6 933
			.64	Climb	100	6 333	
			.64	Climb	100	6 655	
			.34	Climb	Basic	7 211	
			(g)	Climb	Basic	7 222	
			.64	Climb	100	7 603	
	241	-120	0.44	Climb	5	3 910	4 642
			.34	Climb	Basic	3 943	
			.44	Climb	5	4 258	
			.44	Climb	5	5 025	
			.64	Climb	100	5 409	
			.84	Climb	1 000	6 353	

[a]Median of six.

[b]Median of five.

[c]Test in progress.

[d]Test was terminated.

[e]Maximum temperature in each flight was 616 K.

[f]Test in progress, no failures.

[g]Not recorded.

TABLE IV.- FATIGUE LIVES FROM REAL-TIME TESTS – Continued

(a) Duplex-annealed Ti-8Al-1Mo-1V titanium-alloy sheet, 1.27 mm thick – Concluded

Stress sequence	Design mean stress, MN/m^2	Minimum stress for GAG cycles, MN/m^2	Specimen failed at –			Fatigue life, flights	
			θ	Segment of flight	Kind of flight	Individual	Median (a)
[h]A	172	-86	0.44	Climb	5	9 228	[c]>17 398
			.34	Climb	Basic	12 293	
			.34	Climb	Basic	17 398	
			(c)	(c)	(c)	[c]>17 398	
			(c)	(c)	(c)	[c]>17 398	
			(c)	(c)	(c)	[c]>17 398	
	207	-104	0.74	Climb	1000	4 151	5 254
			.44	Climb	5	4 519	
			.84	Climb	1000	5 212	
			.44	Climb	5	5 295	
			.74	Climb	1000	6 264	
			.74	Climb	1000	6 264	
	241	-120	0.64	Climb	100	3 441	4 462
			.54	Climb	100	4 426	
			.44	Climb	5	4 457	
			.44	Climb	5	4 467	
			.44	Climb	5	4 472	
			.54	Climb	100	5 098	
C	172	-86	(f)	(f)	(f)	(f)	(f)
	207	-104	0.34	Climb	Basic	8 605	11 981
			.44	Climb	5	10 368	
			.14	Cruise	Basic	10 704	
			.34	Cruise	100	13 258	
			.14	Cruise	Basic	18 244	
			0	Cruise	Basic	25 403	
	241	-120	0.34	Cruise	100	5 837	6 486
			.14	Cruise	Basic	6 312	
			.24	Cruise	100	6 457	
			0	Cruise	Basic	6 514	
			0	Cruise	Basic	9 547	
			.44	Cruise	5	14 446	
E_0	241	0	0.74	Climb	1000	6 238	7 839
			.44	Climb	5	6 769	
			.44	Climb	5	7 836	
			.44	Climb	5	7 842	
			.24	Climb	Basic	8 501	
			.54	Climb	100	9 263	

[a]Median of six.

[c]Test in progress.

[f]Test in progress, no failures.

[h]Maximum temperature in each flight was 616 K, and salt was applied to specimens once each work day.

TABLE IV.- FATIGUE LIVES FROM REAL-TIME TESTS – Concluded

(b) Annealed Ti-6Al-4V titanium-alloy sheet, 1.02 mm thick

Stress sequence	Design mean stress, MN/m^2	Minimum stress for GAG cycles, MN/m^2	Specimen failed at –			Fatigue life, flights	
			θ	Segment of flight	Kind of flight	Individual	Median (a)
A	172	-86	---	-----	-----	--------	(b)
	207	-104	0.54	Climb	1000	11 452	16 090
			.14	Climb	5	13 879	
			.44	Climb	5	13 962	
			.64	Climb	100	18 217	
			.34	Climb	Basic	18 464	
			(c)	(c)	(c)	[c]>22 242	
	241	-120	0.34	Climb	Basic	5 054	5 697
			.44	Climb	5	5 203	
			.44	Climb	5	5 660	
			.64	Climb	100	5 734	
			.44	Climb	5	5 842	
			.64	Climb	100	6 875	

[a]Median of six.

[b]Test in progress, no failures.

[c]Test was terminated.

(c) Solution treated and aged Ti-6Al-4V titanium-alloy sheet, 1.27 mm thick

Stress sequence	Design mean stress, MN/m^2	Minimum stress for GAG cycles, MN/m^2	Specimen failed at –			Fatigue life, flights	
			θ	Segment of flight	Kind of flight	Individual	Median (a)
A	172	-86	0.54	Climb	100	11 030	[b]>11 030
	207	-104	0.54	Climb	1000	7 310	8 433
			.54	Climb	100	7 811	
			.64	Climb	100	8 123	
			.54	Climb	100	8 743	
			.54	Climb	100	9 252	
			.54	Climb	100	11 655	
	241	-120	0.74	Climb	1000	4 165	5 100
			.14	Descent	5	4 650	
			.44	Climb	5	5 061	
			.44	Climb	5	5 139	
			.44	Climb	5	5 738	
			.14	Climb	100	7 186	

[a]Median of six.

[b]Test in progress.

TABLE V.- FATIGUE LIVES FROM ACCELERATED TESTS

AT ROOM TEMPERATURE

[Notched specimens, K_{exp} = 4.1]

(a) Duplex-annealed Ti-8Al-1Mo-1V titanium-alloy sheet, 1.27 mm thick

Stress sequence	Design mean stress, MN/m^2	Minimum stress for GAG cycles, MN/m^2	Specimen failed at –			Fatigue life, flights	
			θ	Segment of flight	Kind of flight	Individual	Median
A	172	-86	0.44	Climb	Basic	30 353	51 249
			.64	Climb	100	41 561	
			.84	Climb	1000	42 707	
			.44	Climb	5	43 587	
			.44	Climb	5	47 759	
			.64	Climb	100	50 311	
			.54	Climb	100	52 186	
			.54	Climb	100	74 894	
			.44	Climb	5	102 655	
			.34	Climb	Basic	107 659	
			.54	Climb	100	124 061	
			.24	Climb	Basic	153 386	
			(a)	(a)	(a)	[b]>52 000	
			(a)	(a)	(a)	[b]>52 000	
			(a)	(a)	(a)	[b]>52 000	
			(a)	(a)	(a)	[b]>52 000	
	207	-104	(c)	(c)	(c)	12 770	14 800
			0.24	Climb	5	13 400	
			.44	Climb	5	13 900	
			.64	Climb	100	14 800	
			.24	Climb	Basic	16 600	
			(c)	(c)	(c)	17 560	
			.24	Climb	Basic	33 300	
	241	-120	0.44	Climb	5	5 800	7 270
			.44	Climb	5	6 420	
			.44	Climb	5	6 540	
			(c)	(c)	(c)	7 070	
			(c)	Climb	1000	7 270	
			.44	Climb	5	7 520	
			.44	Climb	5	7 850	
			(c)	Climb	5	7 950	
			.84	Climb	1000	8 300	

[a]Specimen did not fail.

[b]Test was terminated. Data not included in median value.

[c]Not recorded.

TABLE V.- FATIGUE LIVES FROM ACCELERATED TESTS

AT ROOM TEMPERATURE – Continued

(a) Duplex-annealed Ti-8Al-1Mo-1V titanium-alloy sheet, 1.27 mm thick – Continued

Stress sequence	Design mean stress, MN/m^2	Minimum stress for GAG cycles, MN/m^2	Specimen failed at –			Fatigue life, flights	
			θ	Segment of flight	Kind of flight	Individual	Median
C	172	-86	0.84	Climb	1000	17 700	22 100
			.14	Cruise	Basic	19 200	
			.14	Cruise	5	20 290	
			.14	Cruise	Basic	22 100	
			.44	Climb	5	26 700	
			.14	Cruise	5	27 983	
			.14	Cruise	Basic	40 940	
	207	-104	0.14	Cruise	Basic	8 410	10 275
			.14	Cruise	Basic	8 450	
			(c)	Climb	Basic	8 950	
			.24	Cruise	100	11 600	
			.14	Cruise	Basic	14 930	
			.14	Cruise	Basic	15 330	
	241	-120	(c)	Climb	Basic	5 150	5 539
			0.14	Cruise	5	5 220	
			.14	Cruise	5	5 428	
			.14	Cruise	Basic	5 650	
			.24	Cruise	5	5 920	
			.14	Cruise	Basic	6 340	

[c]Not recorded.

TABLE V.- FATIGUE LIVES FROM ACCELERATED TESTS

AT ROOM TEMPERATURE – Continued

(a) Duplex-annealed Ti-8Al-1Mo-1V titanium-alloy sheet, 1.27 mm thick – Continued

Stress sequence	Design mean stress, MN/m^2	Minimum stress for GAG cycles, MN/m^2	Specimen failed at –			Fatigue life, flights	
			θ	Segment of flight	Kind of flight	Individual	Median
E	172	-172	0.44	Climb	5	18 450	22 165
			.94	Climb	10 000	20 832	
			.54	Climb	100	22 040	
			.54	Climb	100	22 290	
			.54	Climb	100	29 600	
			.44	Climb	5	33 280	
	207	0	0.54	Climb	100	28 700	>52 000
			.14	Climb	Basic	42 430	
			(a)	(a)	(a)	[a]>52 000	
			(a)	(a)	(a)	[a]>52 000	
			(a)	(a)	(a)	[a]>52 000	
			(a)	(a)	(a)	[a]>52 000	
	207	-207	0.14	Climb	100	7 100	8 350
			.14	Climb	5	7 100	
			.14	Climb	1 000	7 300	
			.14	Climb	5	9 400	
			.44	Climb	5	9 556	
			.14	Climb	Basic	12 800	
	241	0	0.64	Climb	100	8 748	9 832
			(c)	(c)	(c)	8 770	
			.64	Climb	100	8 957	
			.84	Climb	1 000	9 373	
			.44	Climb	5	10 290	
			.44	Climb	5	11 321	
			.54	Climb	100	13 853	
			.44	Climb	5	14 327	
	241	-241	0.54	Climb	1 000	4 165	5 223
			.64	Climb	100	4 582	
			.44	Climb	5	4 858	
			.44	Climb	5	5 587	
			.44	Climb	5	5 681	
			.44	Climb	5	5 686	

[a]Specimen did not fail.

[c]Not recorded.

TABLE V.- FATIGUE LIVES FROM ACCELERATED TESTS

AT ROOM TEMPERATURE – Continued

(a) Duplex-annealed Ti-8Al-1Mo-1V titanium-alloy sheet, 1.27 mm thick – Concluded

Stress sequence	Design mean stress, MN/m^2	Minimum stress for GAG cycles, MN/m^2	Specimen failed at –			Fatigue life, flights	
			θ	Segment of flight	Kind of flight	Individual	Median
[d]F	172	-86	0.44 .24 (a)	Climb Climb (a)	100 5 (a)	66 460 106 200 [a]>200 000	106 200
	207	-104	0.64 .24 .24	Climb Climb Climb	100 100 Basic	19 440 22 150 22 540	22 150
	241	-120	0.24 .24 .74	Climb Climb Climb	100 Basic 1000	8 840 9 650 12 470	9 650
G	172	-86	0.64 .34 .34	(e) (e) (e)	100 Basic Basic	69 580 111 380 120 390	111 380
	207	-104	0.44 .64 .34	(e) (e) (e)	5 100 Basic	28 870 44 930 53 460	44 930
	241	-120	0.44 .34 .64	(e) (e) (e)	5 Basic 100	17 440 18 860 20 380	18 860

[a]Specimen did not fail.

[d]Cycle of largest amplitude (θ = 0.44) was inadvertently omitted from 5th flights.

[e]Type-G stress sequences contained only 1 cycle per flight.

TABLE V.- FATIGUE LIVES FROM ACCELERATED TESTS

AT ROOM TEMPERATURE – Continued

(b) Annealed Ti-6Al-4V titanium-alloy sheet, 1.02 mm thick

Stress sequence	Design mean stress, MN/m^2	Minimum stress for GAG cycles, MN/m^2	Specimen failed at –			Fatigue life, flights	
			θ	Segment of flight	Kind of flight	Individual	Median
A	172	-86	0.54	Climb	5	25 103	61 722
			.44	Climb	5	26 535	
			.44	Climb	5	41 597	
			.44	Climb	5	81 847	
			.44	Climb	5	115 483	
			(a)	(a)	(a)	[a]>125 000	
	207	-104	0.24	Climb	5	10 230	13 220
			.34	Climb	Basic	11 600	
			.14	Climb	5	12 300	
			.54	Climb	100	14 140	
			.14	Climb	Basic	19 260	
			.24	Climb	10 000	20 800	
	241	-120	0.54	Climb	100	4 680	6 280
			.14	Climb	Basic	4 930	
			.84	Climb	1 000	6 250	
			.44	Climb	5	6 310	
			.34	Climb	Basic	7 000	
			.64	Climb	100	8 200	

[a]Specimen did not fail.

TABLE V.- FATIGUE LIVES FROM ACCELERATED TESTS
AT ROOM TEMPERATURE – Concluded

(c) Solution treated and aged Ti-6Al-4V titanium-alloy sheet, 1.27 mm thick

Stress sequence	Design mean stress, MN/m^2	Minimum stress for GAG cycles, MN/m^2	Specimen failed at –			Fatigue life, flights	
			θ	Segment of flight	Kind of flight	Individual	Median
A	172	-86	0.44	Climb	5	29 123	90 988
			.74	Climb	1 000	35 415	
			.44	Climb	5	76 655	
			.44	Climb	5	105 321	
			.34	Climb	Basic	157 661	
			(a)	(a)	(a)	[a]>380 000	
	207	-104	0.14	Climb	Basic	8 740	11 870
			.14	Climb	5	11 540	
			.34	Climb	Basic	11 810	
			.14	Climb	5	11 930	
			.74	Climb	1 000	13 520	
			.54	Climb	100	16 120	
	241	-120	0.44	Climb	5	4 140	6 160
			.54	Climb	100	5 100	
			.44	Climb	5	5 710	
			.14	Climb	5	6 610	
			.44	Climb	5	6 830	
			.24	Climb	Basic	7 170	
F	172	-86	0.34	Climb	Basic	35 914	68 748
			.74	Climb	1 000	68 748	
			.34	Climb	Basic	129 231	
	207	-104	0.54	Climb	100	18 228	18 748
			.44	Climb	5	18 504	
			.74	Climb	1 000	18 748	
			.84	Climb	1 000	19 790	
			1.04	Climb	10 000	20 832	
	241	-120	0.54	Climb	100	7 707	10 416
			.94	Climb	10 000	10 416	
			1.04	Climb	10 000	10 416	
G	172	-86	0.84	(b)	1 000	77 082	98 077
			.64	(b)	100	93 019	
			.44	(b)	5	93 285	
			.44	(b)	5	102 868	
			.34	(b)	Basic	119 590	
			.84	(b)	1 000	443 748	
	207	-104	0.44	(b)	5	33 847	62 186
			.64	(b)	100	45 623	
			.64	(b)	100	62 186	
			.34	(b)	Basic	64 583	
			.84	(b)	1 000	70 832	
	241	-120	0.44	(b)	5	15 394	16 663
			.34	(b)	Basic	16 663	
			.44	(b)	5	16 847	

[a]Specimen did not fail.

[b]Type-G stress sequences contained only 1 cycle per flight.

TABLE VI.- FATIGUE LIVES FROM ACCELERATED TESTS AT 561 K

[Notched specimens, $K_{exp} = 4.1$]

(a) Duplex-annealed Ti-8Al-1Mo-1V titanium-alloy sheet, 1.27 mm thick

Stress sequence	Design mean stress, MN/m^2	Minimum stress for GAG cycles, MN/m^2	Specimen failed at –			Fatigue life, flights	
			θ	Segment of flight	Kind of flight	Individual	Median
A	172	-86	0.34	Climb	1 000	17 680	33 270
			.24	Climb	5	18 160	
			.44	Climb	5	32 500	
			.14	Climb	Basic	34 040	
			.14	Climb	5	42 700	
			(a)	(a)	(a)	[a]>52 000	
	207	-104	0.64	Climb	100	6 450	7 015
			.44	Climb	(b)	6 830	
			.44	Climb	5	6 900	
			.14	Climb	5	7 130	
			.44	Climb	100	7 490	
			.44	Climb	5	7 550	
	241	-120	0.44	Climb	5	2 670	3 715
			.44	Climb	5	3 260	
			.24	Climb	100	3 530	
			.24	Climb	5	3 900	
			.34	Climb	Basic	4 110	
			.14	Climb	5	4 350	
C	172	-86	0.24	Cruise	5	11 108	15 456
			.24	Cruise	5	12 655	
			.64	Climb	100	12 811	
			.14	Cruise	Basic	18 100	
			.14	Climb	Basic	19 200	
			.14	Cruise	5	19 600	
	207	-104	0.14	Cruise	5	3 360	5 400
			.14	Cruise	Basic	5 090	
			.14	Cruise	Basic	5 300	
			.14	Cruise	100	5 500	
			.14	Cruise	Basic	5 800	
			.64	Climb	100	6 420	
	241	-120	0.14	Cruise	Basic	1 850	2 840
			.24	Cruise	5	2 410	
			.14	Cruise	Basic	2 800	
			.24	Cruise	5	2 880	
			.24	Cruise	Basic	3 360	
			.24	Cruise	5	3 450	

[a]Specimen did not fail.

[b]Not recorded.

TABLE VI.- FATIGUE LIVES FROM ACCELERATED TESTS AT 561 K – Continued

(a) Duplex-annealed Ti-8Al-1Mo-1V titanium-alloy sheet, 1.27 mm thick – Continued

Stress sequence	Design mean stress, MN/m^2	Minimum stress for GAG cycles, MN/m^2	Specimen failed at –			Fatigue life, flights	
			θ	Segment of flight	Kind of flight	Individual	Median
E	172	0	0.84	Climb	1 000	22 914	36 482
			.64	Climb	100	34 269	
			.44	Climb	5	38 696	
			(a)	(a)	(a)	[a]>38 700	
	172	-172	1.14	Climb	10 000	10 416	11 061
			1.14	Climb	10 000	10 416	
			.64	Climb	100	10 936	
			.44	Climb	5	11 186	
			.44	Climb	5	11 785	
			.44	Climb	5	14 940	
	207	0	0.14	Climb	5	7 370	24 400
			.64	Climb	100	9 200	
			1.04	Climb	10 000	20 800	
			.64	Climb	100	28 000	
			.74	Climb	1 000	48 800	
			(a)	(a)	(a)	[a]>52 000	
	207	-207	0.14	Climb	Basic	3 780	5 850
			.44	Climb	5	4 100	
			.24	Climb	Basic	5 850	
			.64	Climb	100	6 040	
			.44	Climb	5	6 129	
	241	0	0.44	Climb	5	5 509	5 676
			.64	Climb	100	5 519	
			.64	Climb	100	5 623	
			.64	Climb	100	5 728	
			.54	Climb	100	5 936	
			.64	Climb	100	5 936	
	241	-241	0.44	Climb	5	2 327	2 707
			.14	Climb	5	2 676	
			.14	Climb	100	2 707	
			.54	Climb	100	2 707	
			.44	Climb	5	2 873	
			.74	Climb	1 000	3 123	

[a]Specimen did not fail.

TABLE VI.- FATIGUE LIVES FROM ACCELERATED TESTS AT 561 K – Continued

(a) Duplex-annealed Ti-8Al-1Mo-1V titanium-alloy sheet, 1.27 mm thick – Concluded

Stress sequence	Design mean stress, MN/m^2	Minimum stress for GAG cycles, MN/m^2	Specimen failed at –			Fatigue life, flights	
			θ	Segment of flight	Kind of flight	Individual	Median
F	172	-86	0.64	Climb	100	19 478	21 561
			.94	Climb	10 000	20 832	
			.54	Climb	100	21 561	
			.44	Climb	5	21 644	
			.44	Climb	5	25 290	
	207	-104	0.74	Climb	1 000	8 332	10 572
			.54	Climb	100	10 103	
			.64	Climb	100	11 040	
			.54	Climb	100	11 873	
	241	-120	0.44	Climb	5	6 222	6 456
			.74	Climb	1 000	6 248	
			.54	Climb	100	6 665	
			.64	Climb	100	6 769	
G	172	-86	1.14	(c)	10 000	52 000	54 350
			.44	(c)	5	54 350	
			.44	(c)	5	54 780	
	207	-104	0.64	(c)	100	21 220	21 530
			.64	(c)	100	21 530	
			.44	(c)	5	22 850	
	241	-120	0.34	(c)	Basic	10 414	10 416
			1.14	(c)	10 000	10 416	
			1.14	(c)	10 000	10 416	

[c]Type-G stress sequences contained only 1 cycle per flight.

TABLE VI.- FATIGUE LIVES FROM ACCELERATED TESTS AT 561 K – Continued

(b) Annealed Ti-6Al-4V titanium-alloy sheet, 1.02 mm thick

Stress sequence	Design mean stress, MN/m^2	Minimum stress for GAG cycles, MN/m^2	Specimen failed at –			Fatigue life, flights	
			θ	Segment of flight	Kind of flight	Individual	Median
A	172	-86	0.34	Climb	Basic	14 600	19 186
			.44	Climb	5	15 363	
			.34	Climb	Basic	18 581	
			.74	Climb	100	19 790	
			.94	Climb	10 000	20 832	
			.44	Climb	5	25 452	
	207	-104	0.24	Climb	5	5 750	6 555
			.14	Climb	100	6 050	
			.14	Climb	Basic	6 180	
			.34	Climb	Basic	6 930	
			.14	Climb	100	7 350	
			.44	Climb	5	7 580	
	241	-120	0.14	Climb	1 000	2 080	3 340
			.14	Climb	Basic	2 870	
			.14	Climb	5	3 210	
			.34	Climb	Basic	3 470	
			.14	Climb	Basic	4 060	
			.24	Climb	5	4 730	

TABLE VI.- FATIGUE LIVES FROM ACCELERATED TESTS AT 561 K – Concluded

(c) Solution treated and aged Ti-6Al-4V titanium-alloy sheet, 1.27 mm thick

Stress sequence	Design mean stress, MN/m^2	Minimum stress for GAG cycles, MN/m^2	Specimen failed at –			Fatigue life, flights	
			θ	Segment of flight	Kind of flight	Individual	Median
A	172	-86	0.24	Climb	Basic	8 700	18 922
			.44	Climb	5	13 488	
			.64	Climb	100	18 123	
			.34	Climb	Basic	19 721	
			.44	Climb	5	23 108	
			.14	Climb	5	40 879	
	207	-104	0.44	Climb	5	5 020	5 375
			.14	Climb	Basic	5 070	
			.24	Climb	5	5 150	
			.24	Climb	5	5 600	
			.44	Climb	5	7 500	
			.44	Climb	5	9 600	
	241	-120	0.24	Climb	5	3 150	3 315
			.14	Climb	Basic	3 170	
			.54	Climb	100	3 220	
			.44	Climb	5	3 410	
			.14	Climb	100	3 650	
			.54	Climb	100	3 950	
F	172	-86	0.44	Climb	5	34 129	36 103
			.44	Climb	5	36 103	
			.34	Climb	Basic	47 544	
	207	-104	0.54	Climb	100	10 103	11 946
			.44	Climb	5	11 946	
			.74	Climb	1 000	13 540	
	241	-120	0.44	Climb	5	6 504	7 290
			.84	Climb	1 000	7 290	
			.44	Climb	5	7 702	
G	172	-86	0.84	(a)	1 000	64 582	76 634
			.44	(a)	5	74 525	
			.44	(a)	5	78 743	
			.34	(a)	Basic	210 720	
	207	-104	0.44	(a)	5	27 493	31 248
			1.14	(a)	10 000	31 248	
			1.14	(a)	10 000	31 248	
	241	-120	0.64	(a)	100	13 332	14 373
			.64	(a)	100	14 373	
			.84	(a)	1 000	15 623	

[a]Type-G stress sequences contained only 1 cycle per flight.

TABLE VII.- FATIGUE LIVES FROM ACCELERATED TESTS AT 616 K

[Notched specimens (K_{exp} = 4.1) of duplex-annealed Ti-8Al-1Mo-1V titanium-alloy sheet, 1.27 mm thick]

Stress sequence	Design mean stress, MN/m^2	Minimum stress for GAG cycles, MN/m^2	Specimen failed at –			Fatigue life, flights	
			θ	Segment of flight	Kind of flight	Individual	Median
A	172	-86	1.04	Climb	10 000	10 416	13 871
			.64	Climb	100	10 832	
			.54	Climb	1 000	11 457	
			.44	Climb	5	12 134	
			.44	Climb	5	12 926	
			.44	Climb	5	13 681	
			.54	Climb	100	14 061	
			.54	Climb	1 000	14 582	
			.14	Climb	5	14 983	
			.24	Climb	5	15 400	
			.54	Climb	1 000	16 665	
			.64	Climb	100	53 853	
	207	-104	0.44	Climb	5	5 180	6 890
			.44	Climb	5	5 350	
			.44	Climb	5	6 100	
			.24	Climb	Basic	6 370	
			.14	Climb	Basic	6 500	
			.54	Climb	1 000	7 280	
			.14	Climb	5	7 350	
			.44	Climb	5	7 630	
			.14	Cruise	Basic	8 480	
			.54	Climb	100	8 630	
	241	-120	0.14	Climb	Basic	2 650	3 220
			.14	Climb	Basic	2 810	
			.54	Climb	100	3 020	
			.14	Climb	5	3 060	
			.44	Climb	5	3 110	
			.84	Climb	1 000	3 120	
			.44	Climb	5	3 320	
			.14	Climb	5	3 450	
			0	Climb	Basic	3 520	
			.64	Climb	100	3 530	
			.44	Climb	5	3 580	
			.14	Climb	5	3 620	

TABLE VIII.- SUMMARY OF CUMULATIVE-DAMAGE ANALYSIS BASED ON MEDIAN LIVES

[Specimens were notched (K_{exp} = 4.1), duplex-annealed Ti-8Al-1Mo-1V titanium alloy, 1.27 mm thick]

Stress sequence	$\sum \frac{n}{N}$ at failure			Portion of $\sum \frac{n}{N}$ at failure due to GAG cycles in operational flights			Predicted lives for $\sum \frac{n}{N}$ = 1.0, flights		
	Design mean stress, MN/m^2			Design mean stress, MN/m^2			Design mean stress, MN/m^2		
	172	207	241	172	207	241	172	207	241
Real-time tests									
A	0.25	0.40	0.48	0.22	0.32	0.32	76 220	24 530	10 606
C	(a)	.78	1.06	(a)	.68	.85	43 975	15 274	6 149
E_0	(b)	(b)	.45	(b)	(b)	.23	(b)	(b)	17 553
Accelerated tests at room temperature									
A	0.83	0.61	0.69	0.73	0.48	0.46	76 220	24 528	10 552
C	.61	.62	.68	.57	.53	.49	44 014	16 383	8 215
E_0	(b)	[c]>1.14	.56	(b)	[c]>.80	.29	202 020	45 893	17 498
E_1	.52	.54	.79	.47	.45	.62	42 626	15 337	6 597
F	1.40	.89	.91	1.23	.71	.61	76 220	24 528	10 552
G	1.35	1.60	1.35	1.29	1.45	1.19	82 781	28 217	13 959
Accelerated tests at 561 K									
A	0.49	0.29	0.38	0.45	0.26	0.33	68 634	23 866	9 675
C	.34	.34	.41	.33	.31	.37	45 025	16 205	6 887
E_0	.12	.40	.24	.11	.33	.18	286 533	61 312	23 969
E_1	.31	.45	.47	.29	.43	.41	35 186	12 837	5 747
F	.32	.44	.67	.29	.39	.58	68 634	23 866	9 675
G	.78	.87	1.00	.74	.80	.93	69 930	24 832	10 351

[a]Test in progress.

[b]No test conducted.

[c]Specimens did not fail.

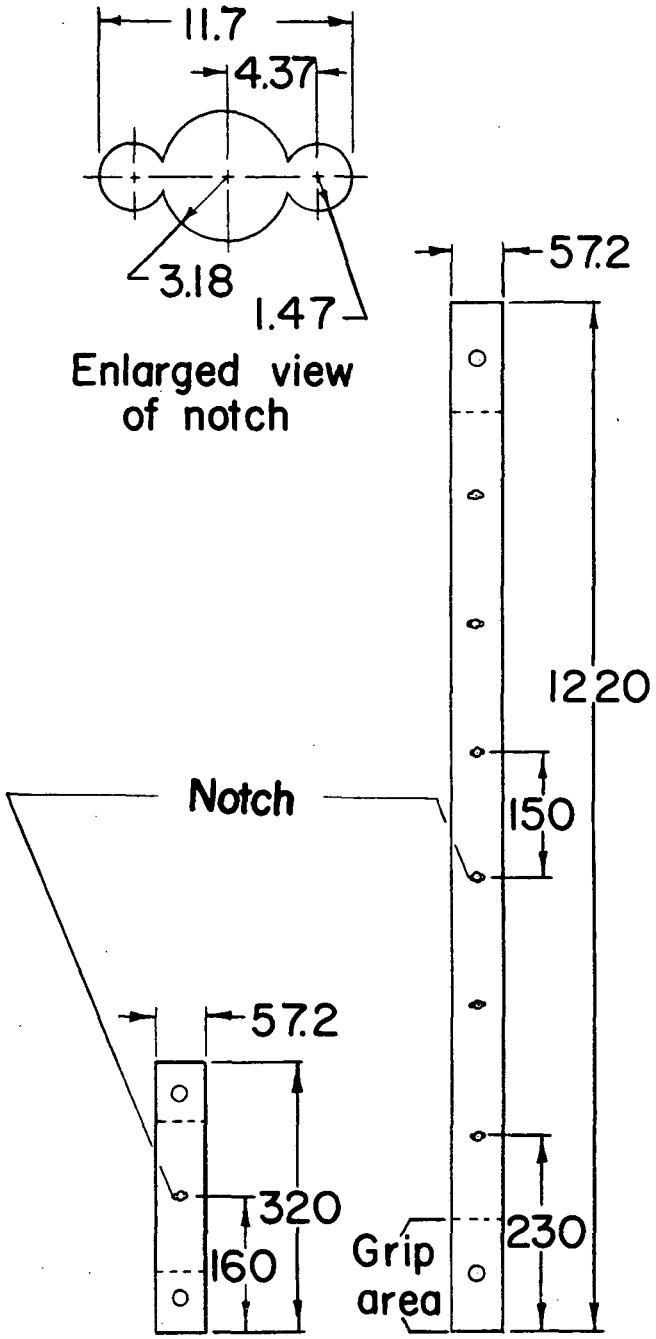

(a) Accelerated tests.

(b) Real-time tests.

Figure 1.- Configurations of fatigue specimens. Dimensions are in millimeters.

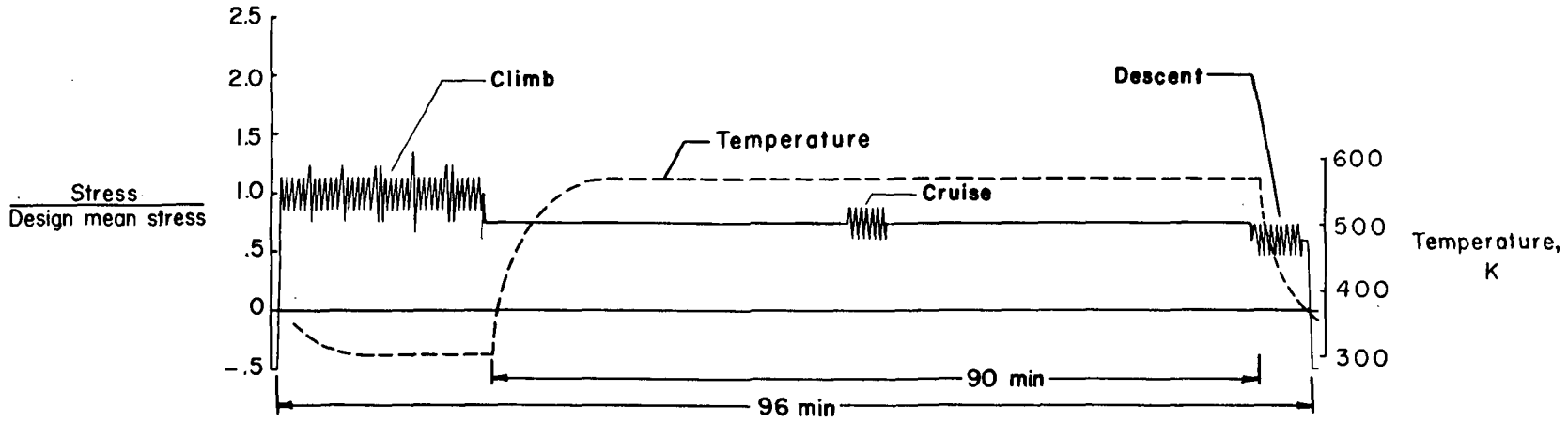

(a) A basic operational flight with cyclic temperature for a real-time test.

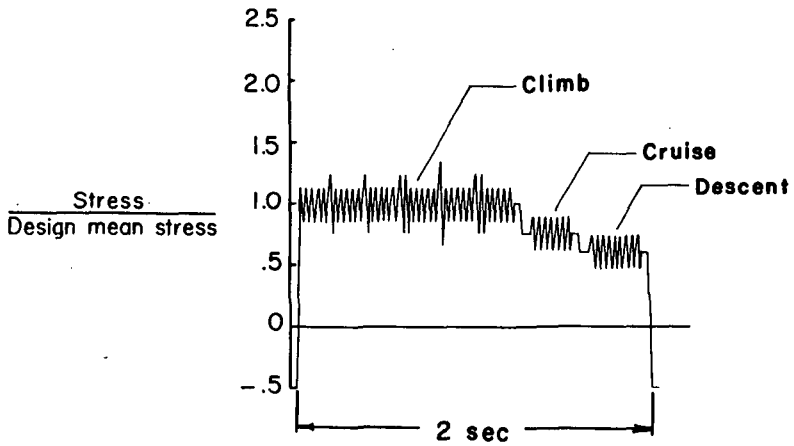

(b) A basic operational flight (constant temperature) for an accelerated test.

Figure 2.- Simulated flights for real-time and accelerated tests.

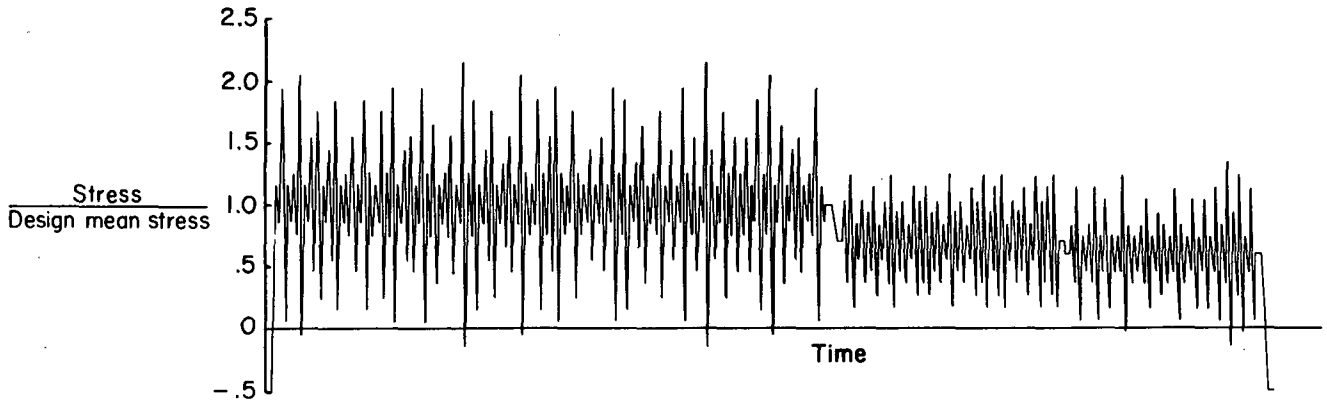

(c) A 10 000th operational flight for an accelerated test.

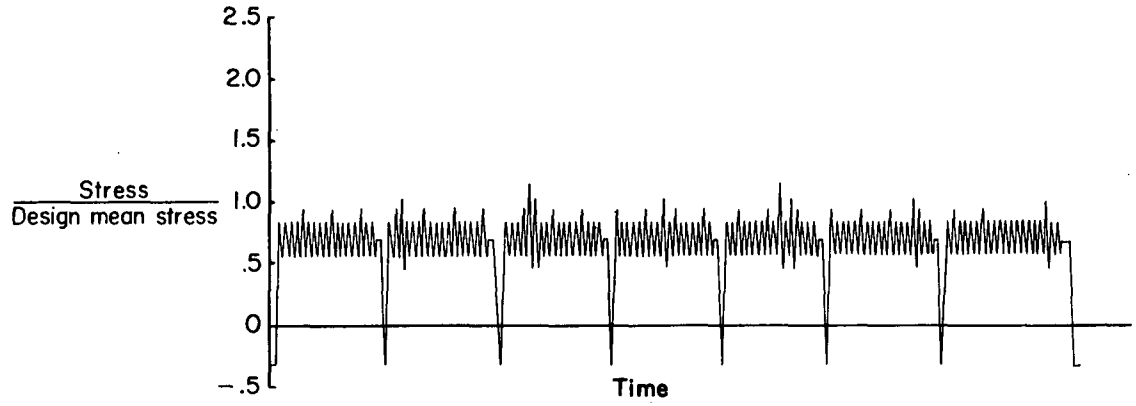

(d) A basic check flight for both real-time and accelerated tests.

Figure 2.- Concluded.

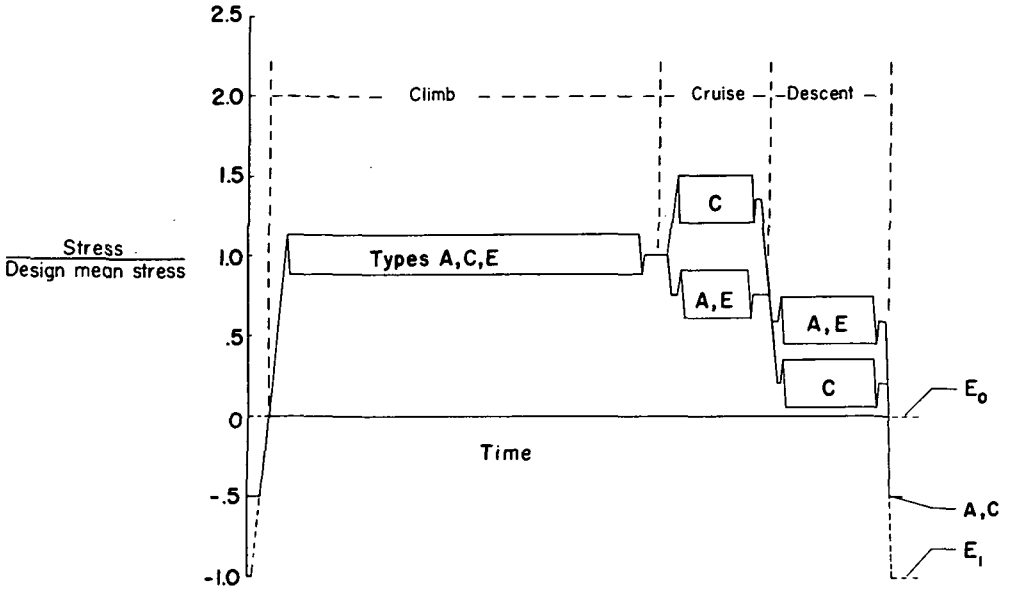

(a) Schematic variations of operational flights.

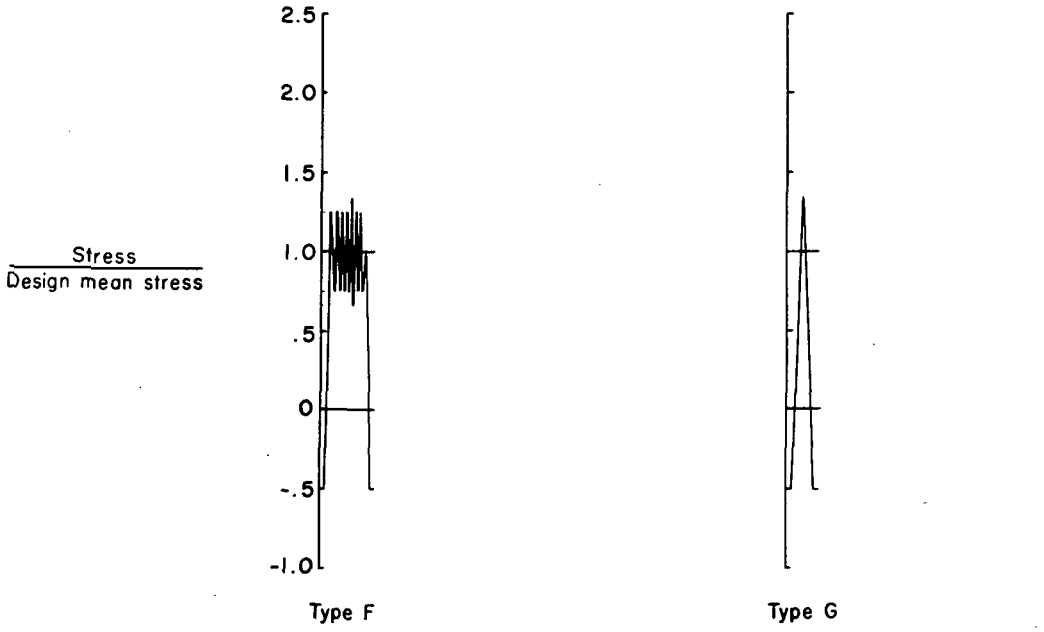

(b) A basic operational flight simplified by omitting all cycles of the smallest amplitude.

(c) A basic operational flight in which only the maximum and minimum stresses are retained.

Figure 3.- Modifications of operational flights.

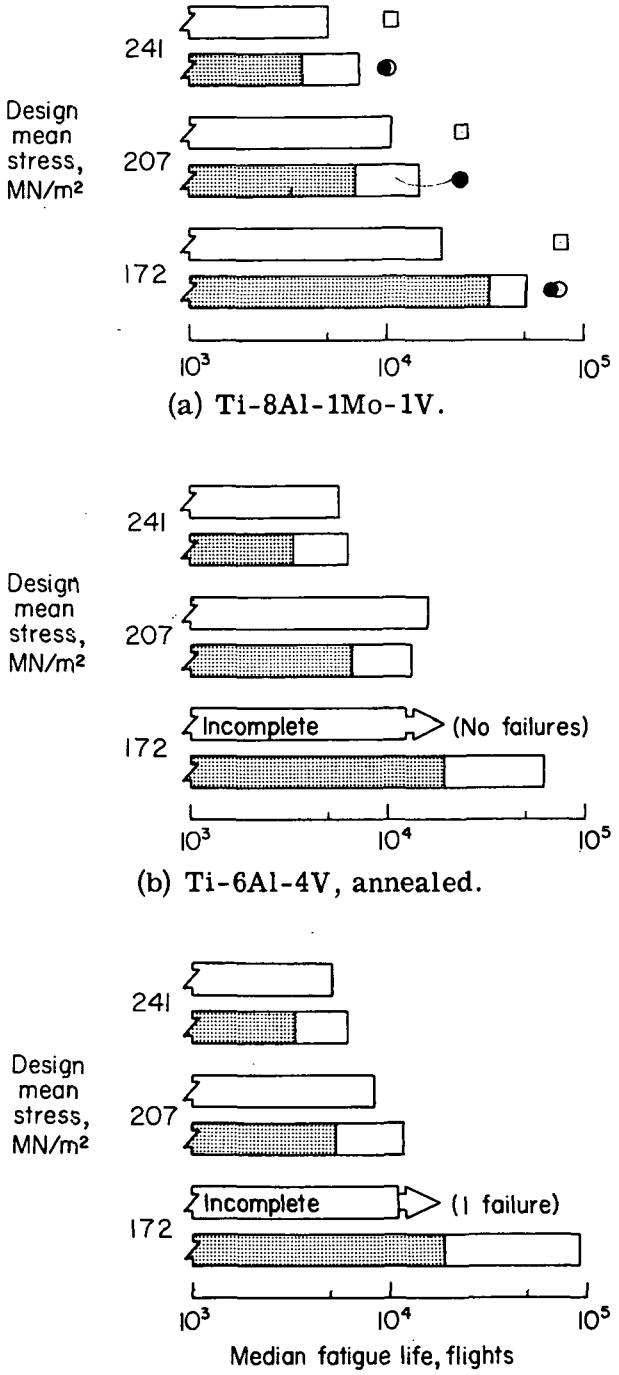

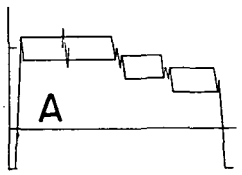

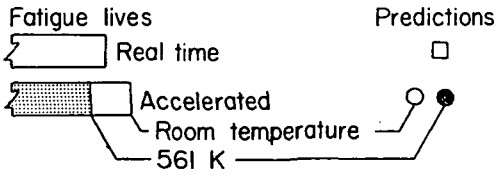

Figure 4.- Results of real-time and accelerated tests with reference (type-A) stress sequences.

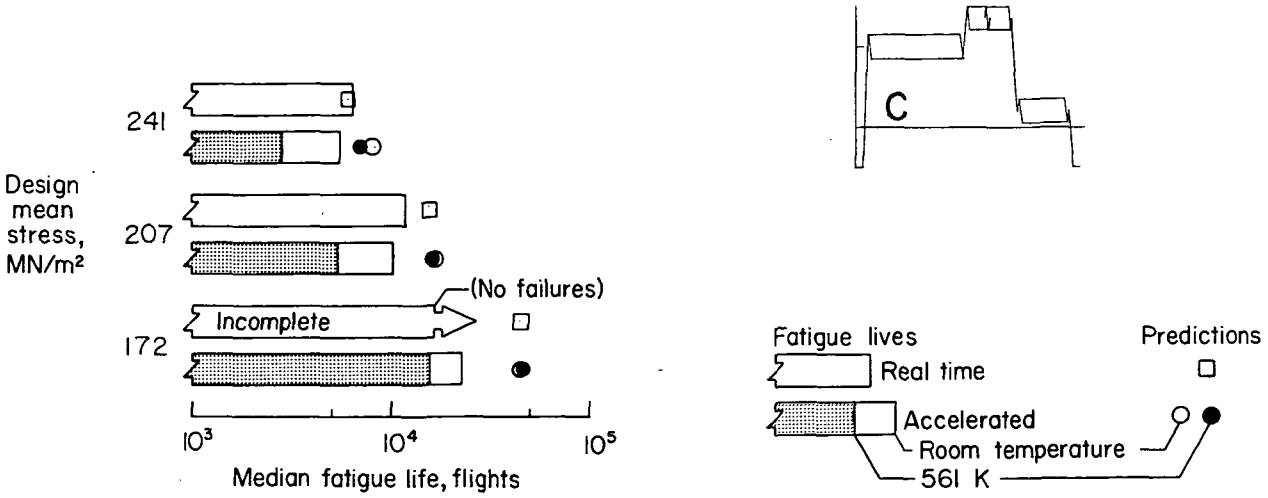

Figure 5.- Effect of simulated thermal stress on fatigue life of Ti-8Al-1Mo-1V in real-time and accelerated tests.

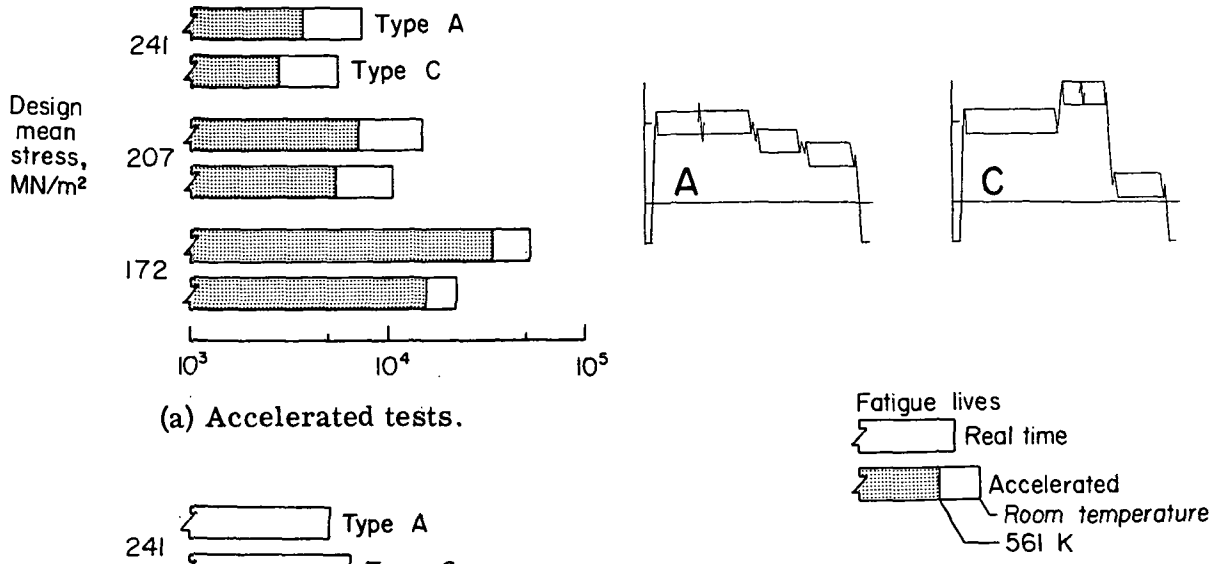

(a) Accelerated tests.

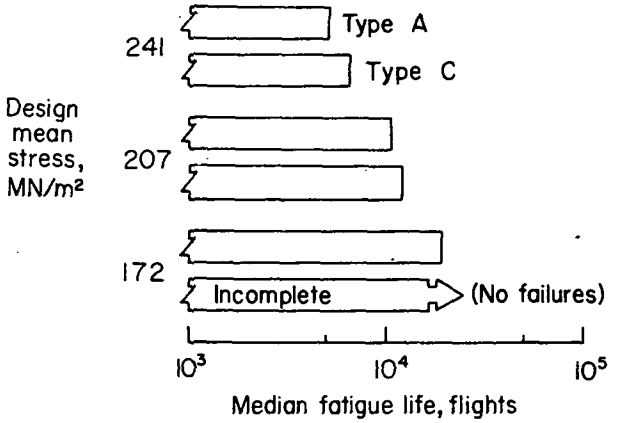

(b) Real-time tests.

Figure 6.- Results of real-time and accelerated fatigue tests of Ti-8Al-1Mo-1V with type-A and type-C stress sequences.

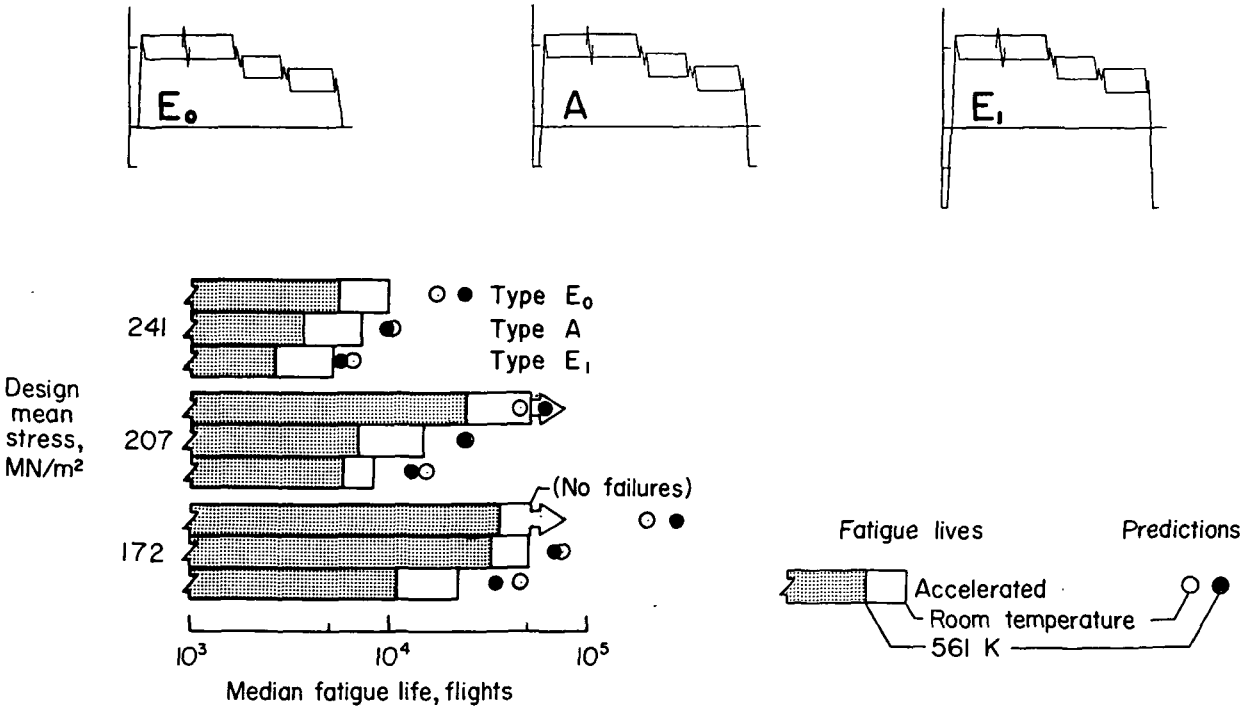

Figure 7.- Effect of minimum stress for ground-air-ground cycles on fatigue life of Ti-8Al-1Mo-1V in accelerated tests.

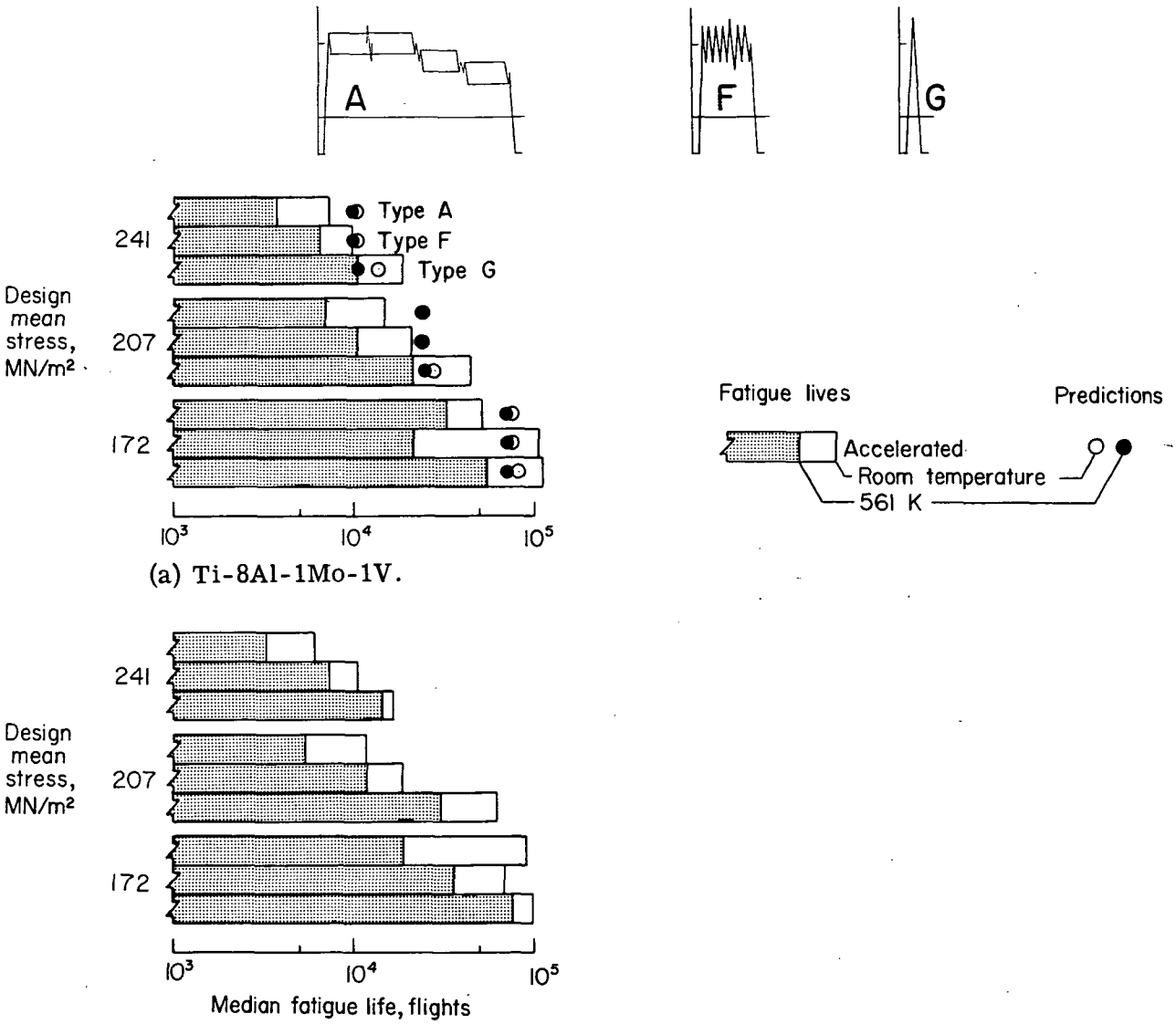

(a) Ti-8Al-1Mo-1V.

(b) Ti-6Al-4V, solution treated and aged.

Figure 8.- Effect of flight simplification on fatigue life of Ti-8Al-1Mo-1V in accelerated tests.

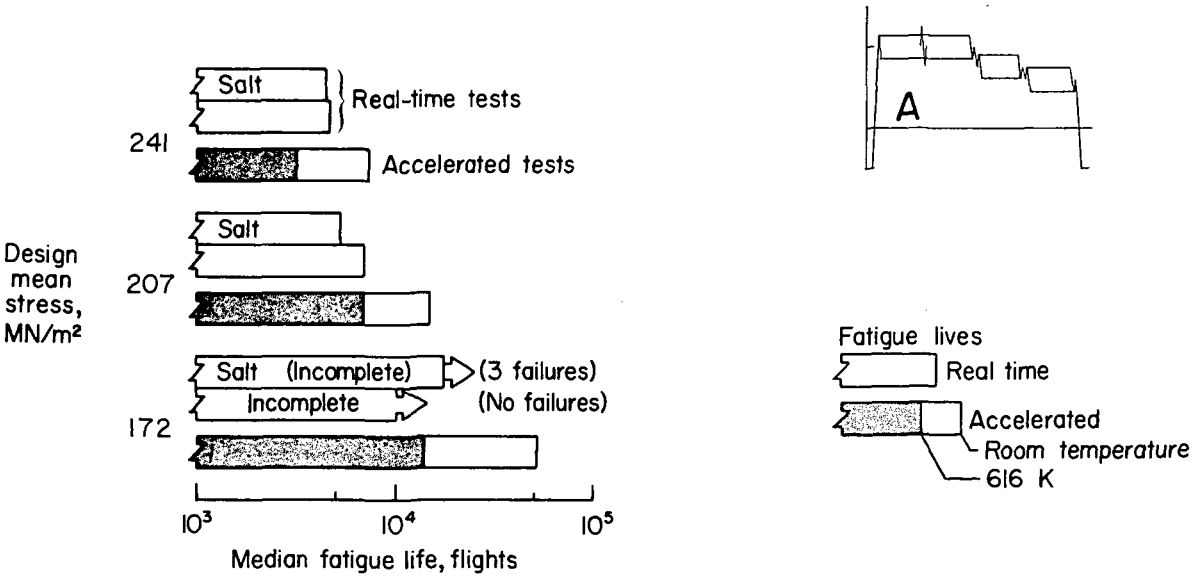

Figure 9.- Effect of salt corrosion on Ti-8Al-1Mo-1V in real-time fatigue tests with a maximum cyclic temperature of 616 K.

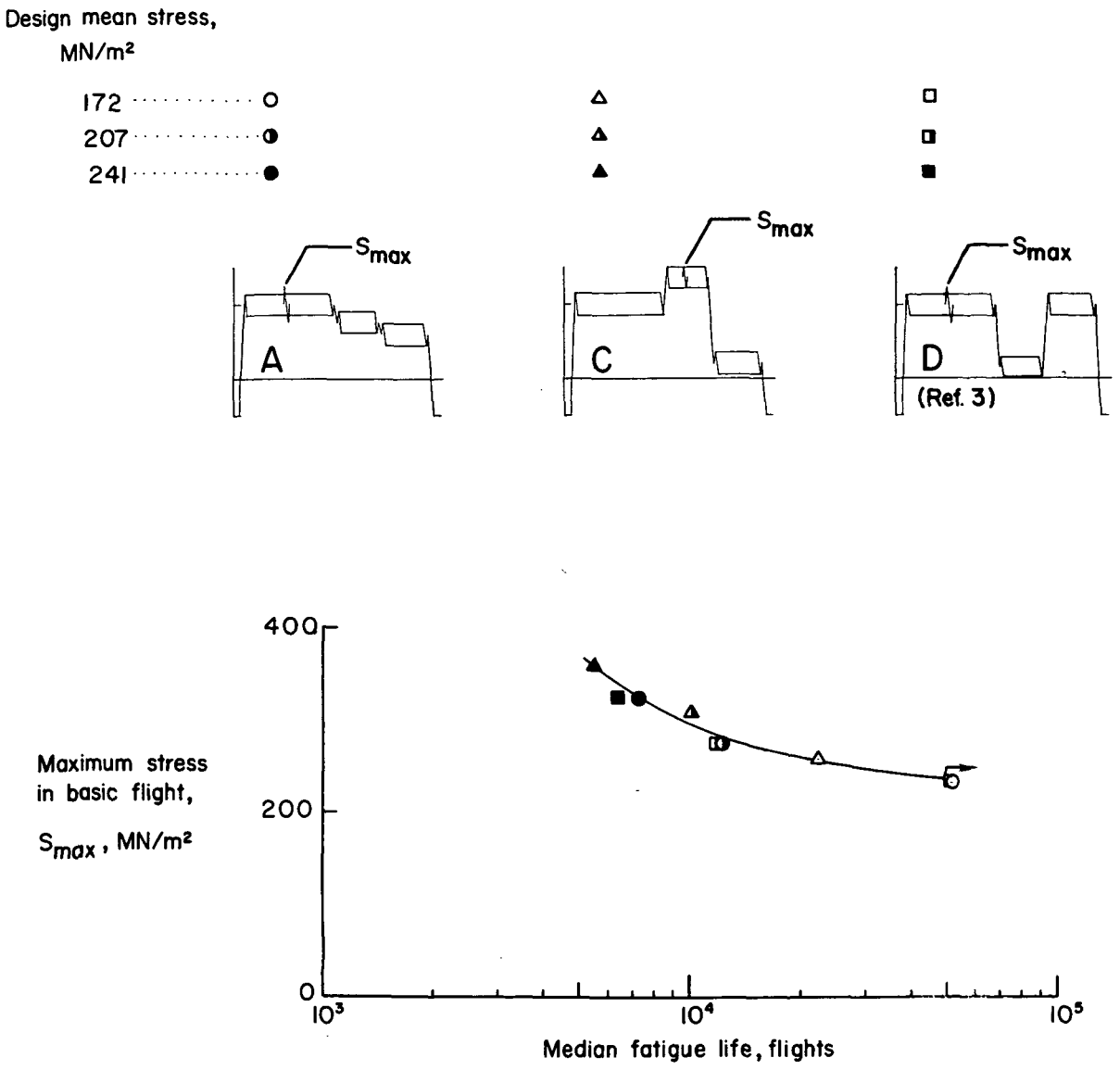

Figure 10.- Effect of maximum flight stress on fatigue life of Ti-8Al-1Mo-1V in accelerated tests at room temperature.

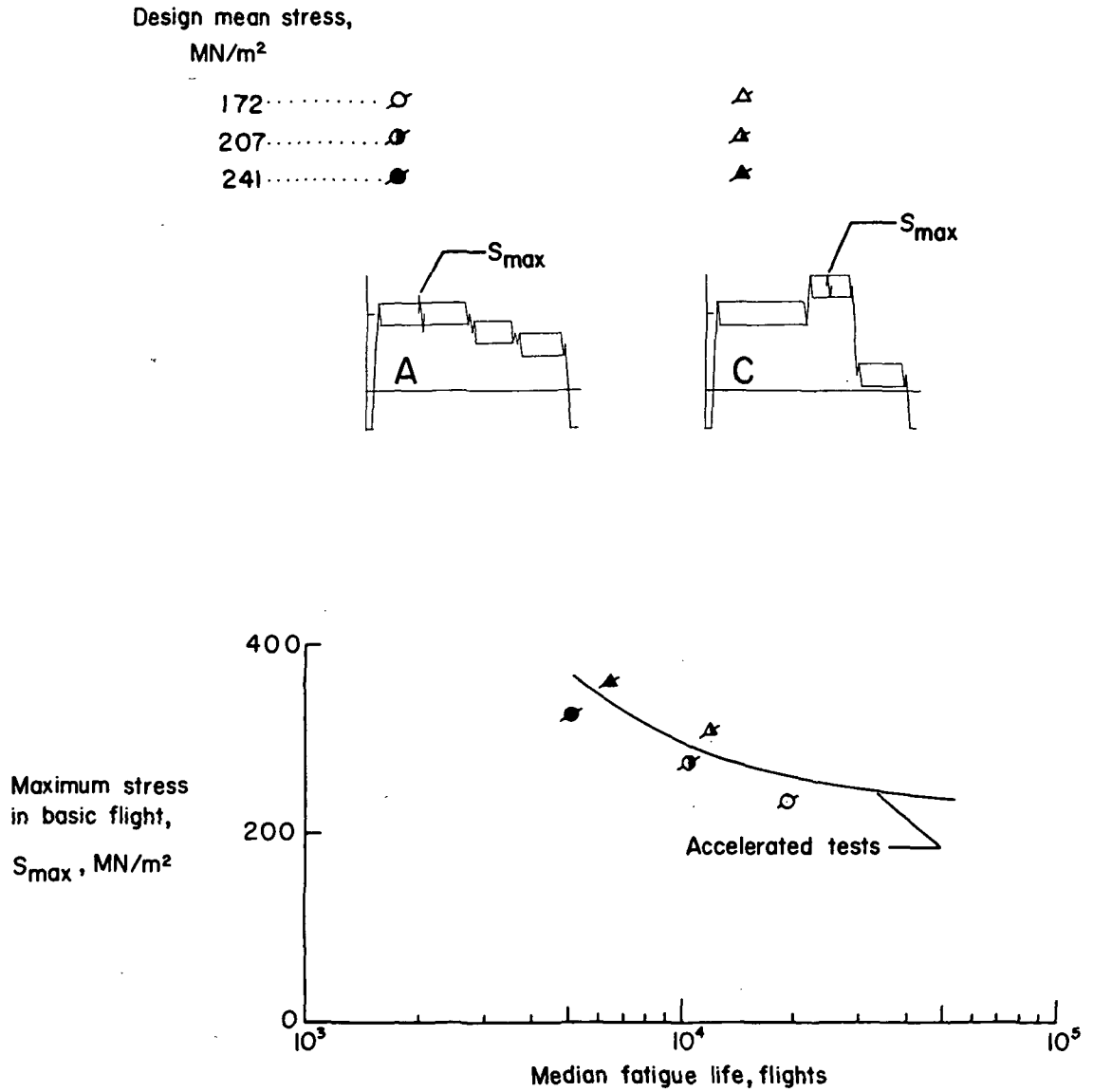

Figure 11.- Correlation of real-time and accelerated test results for Ti-8Al-1Mo-1V.

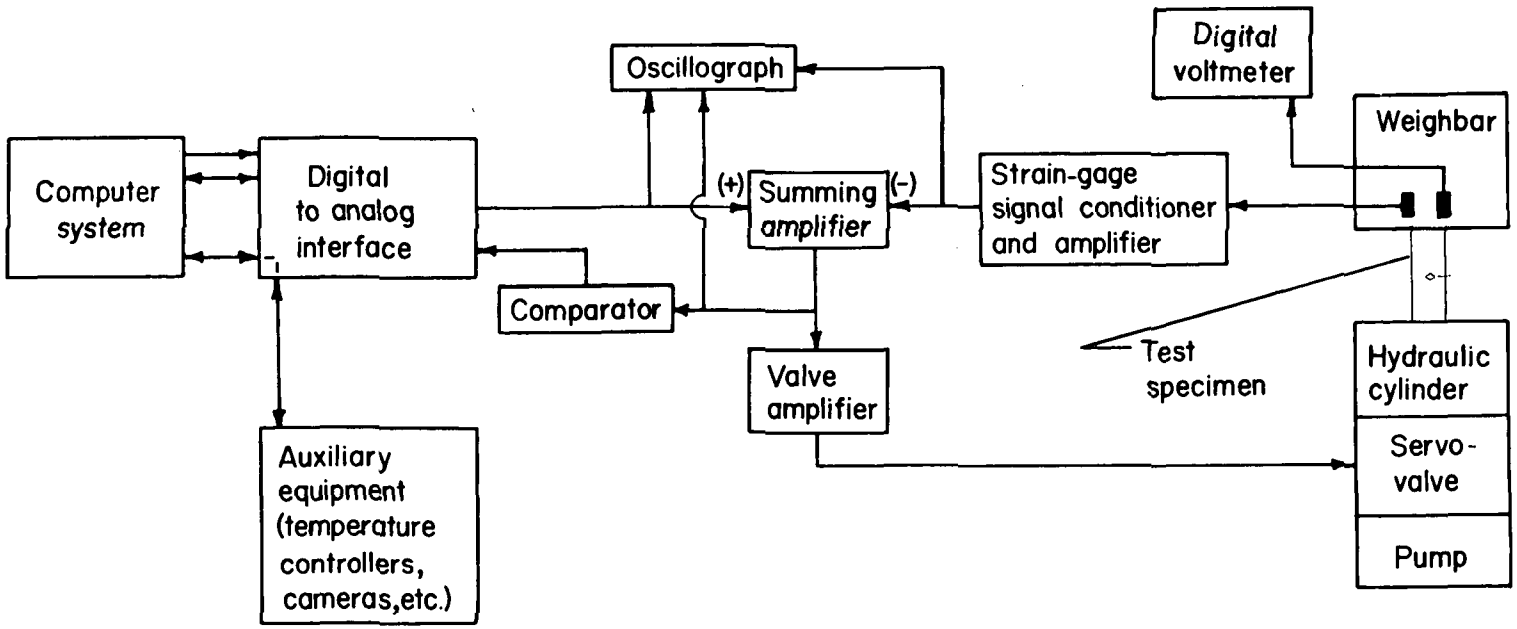

Figure 12.- Schematic diagram of computerized fatigue-testing system used for accelerated tests.

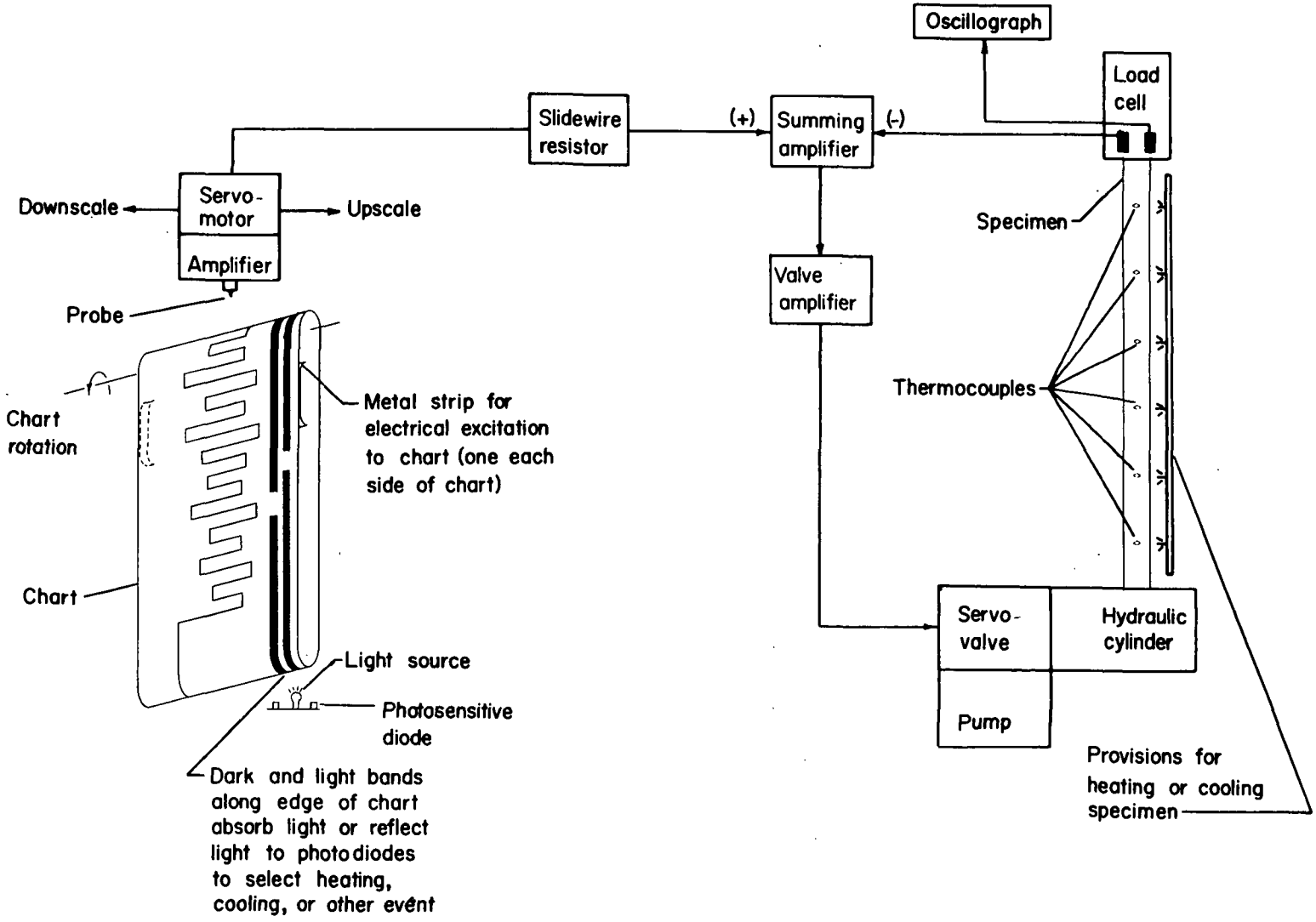

Figure 13.- Schematic diagram of fatigue-testing system used for real-time tests.